Available online at www.sciencedirect.com

ScienceDirect

Nuclear Physics B 954 (2020) 115000

NUCLEAR PHYSICS B

www.elsevier.com/locate/nuclphysb

A comparative study of $0\nu\beta\beta$ decay in symmetric and asymmetric left-right model

Supriya Senapati [a], Chayan Majumdar [a,*], Prativa Pritimita [a], Sudhanwa Patra [b]

[a] *Department of Physics, Indian Institute of Technology Bombay, Powai, Mumbai-400076, India*
[b] *Indian Institute of Technology Bhilai, GEC Campus, Sejbahar, Raipur-492015, Chhattisgarh, India*

Received 4 March 2020; received in revised form 21 March 2020; accepted 22 March 2020
Available online 26 March 2020
Editor: Tommy Ohlsson

Abstract

We study the new physics contributions to neutrinoless double beta decay ($0\nu\beta\beta$) in a TeV scale left-right model with spontaneous D-parity breaking mechanism where the values of the $SU(2)_L$ and $SU(2)_R$ gauge couplings, g_L and g_R are unequal. Neutrino mass is generated in the model via gauge extended inverse seesaw mechanism. We embed the model in a non-supersymmetric $SO(10)$ GUT with a purpose of quantifying the results due to the condition $g_L \neq g_R$. We compare the predicted numerical values of half life of $0\nu\beta\beta$ decay, effective Majorana mass parameter and other lepton number violating parameters for three different cases; (i) for manifest left-right symmetric model ($g_L = g_R$), (ii) for left-right model with spontaneous D parity breaking ($g_L \neq g_R$), (iii) for Pati-Salam symmetry with D parity breaking ($g_L \neq g_R$). We show how different contributions to $0\nu\beta\beta$ decay are suppressed or enhanced depending upon the values of the ratio $\frac{g_R}{g_L}$ that are predicted from successful gauge coupling unification.

* Corresponding author.
E-mail addresses: supriya@phy.iitb.ac.in (S. Senapati), chayan@phy.iitb.ac.in (C. Majumdar), prativa@iitb.ac.in (P. Pritimita), sudhanwa@iitbhilai.ac.in (S. Patra).

https://doi.org/10.1016/j.nuclphysb.2020.115000

1. Introduction

The immediate question that followed the discovery of neutrino mass and mixing by oscillation experiments [1–9] and still remains unanswered is: 'Whether neutrinos are Dirac or Majorana particles?' Even more gripping is the question, 'What gives them such a tiny mass?', since it is believed Higgs mechanism can't be the one responsible. The seesaw mechanism [10–19] which is the minimal approach to explain non-zero neutrino mass presumes them as Majorana fermions. If neutrinos are Majorana fermions [20] they can initiate a very rare process in nature called neutrinoless double beta decay ($0\nu\beta\beta$): ${}^{A}_{Z}X \rightarrow {}^{A}_{Z+2}Y + 2e^{-}$, which clearly violates lepton number by two units [21]. Therefore this process if observed unambiguously can confirm the Majorana nature of neutrinos and total lepton number violation in nature. The detection of this rare phenomena is the main aim of several ongoing experiments that are trying to put a bound on the half life of particular nuclei from which limits on the effective Majorana mass can be obtained easily.

At present, KamLAND-Zen experiment gives the bound on half-life as $T^{0\nu}_{1/2} > 1.6 \times 10^{26}$ yrs using ^{136}Xe [22] while GERDA gives $T^{0\nu}_{1/2} > 8.0 \times 10^{25}$ yrs at 90% C.L. using ^{76}Ge [23]. Translating these limits into effective mass bound it turns out to be $0.26 - 0.6$ eV, whereas the Planck collaboration puts a tight limit on the sum of light neutrino masses to be ≤ 0.23 eV at 95% C.L. [24][1] and as per KATRIN the upper bound on lightest neutrino mass, $m_\beta < 2$ eV at 95% C.L. [28]. Moreover KATRIN is targeted to advance the sensitivity on m_β down to 0.2 eV (90% C.L.) in the near future [29–33]. Which means any positive signal of $0\nu\beta\beta$ decay at the experiments would definitely indicate some new physics contribution to the process.

One possible way to have new physics contributions to $0\nu\beta\beta$ decay process other than the standard mechanism is to study the process in Left-Right Symmetric Model (LRSM) [34–38], which obeys the gauge symmetry $SU(2)_L \times SU(2)_R \times U(1)_{B-L} \times SU(3)_C$. The presence of right-handed neutrino, doubly charged Higgs scalar, and the possibility of left-right mixing can facilitate new decay channels for the process. LRSM has already been exhaustively studied [39–47] in order to explain neutrino mass, lepton number violation, lepton flavor violation, dark matter and baryon asymmetry of the universe. Even rich collider phenomenology is expected when left-right symmetry breaks at TeV scale [48–61].

However a different scenario arises when the discrete parity symmetry (D-parity) of a left-right symmetric theory breaks at a high scale and the local $SU(2)_R$ symmetry breaks at relatively low scale [62,63]. This decoupling of D parity breaking and $SU(2)_R$ symmetry breaking introduces a new scale and as an immediate effect, the gauge couplings for $SU(2)_L$ and $SU(2)_R$ gauge groups become unequal, i.e. $g_L \neq g_R$. In ref. [64] a TeV scale left-right model with D-parity breaking has been studied and in ref. [65] such a model has been embedded in a non-SUSY $SO(10)$ GUT with Pati-Salam symmetry as the highest intermediate breaking step. The same idea has been extended in ref. [66] to study baryon asymmetry of the universe, neutron-antineutron oscillation and proton decay. But the effect of $g_L \neq g_R$ has not been emphasized in these above mentioned works while studying $0\nu\beta\beta$ decay. This deviation ($g_L \neq g_R$) brings a noticeable difference in the $0\nu\beta\beta$ decay sector which is the main essence of this work. We show how different contributions to $0\nu\beta\beta$ decay are suppressed or enhanced depending upon the values of the ratio $\frac{g_R}{g_L}$ that appears in Feynman amplitudes and $\frac{g_L}{g_R}$ that appears in half-life

[1] However, the current cosmological upper limit on the sum of the neutrino masses is a bit tighter than Planck collaboration, ranging from 0.19 eV to 0.12 eV. For more detail discussion on this one may refer refs. [25–27].

estimation. In order to quantify the results due to unequal g_L and g_R we consider two different symmetry breaking chains from non-SUSY SO(10) GUT; one with Pati-Salam symmetry as the highest intermediate step, another without Pati-Salam symmetry [67]. The importance of Pati-Salam symmetry as the highest intermediate step in a $SO(10)$ symmetry breaking chain has already been discussed in ref. [63,68,69].

The rest of the paper is organized as follows. We start our discussion with the basic differences between generic LRSM and asymmetric LRSM and present the symmetry breaking steps in section 2. Next in section 3 we explain how neutrino mass is generated via low scale extended inverse seesaw mechanism in the model. We perform the numerical estimation of different $0\nu\beta\beta$ contributions in section 4 followed by a comparative study of the process in symmetric and asymmetric left-right case in section 5. We summarize our results and conclude in section 6. In appendix A we discuss the new physics contributions to $0\nu\beta\beta$ decay process that arise in a left-right model with spontaneous D parity breaking. We derive upper limits for different lepton number violating parameters in appendix B. We discuss the role of Pati-Salam symmetry in predicting half-life of $0\nu\beta\beta$ decay and other LNV parameters and show the gauge coupling unifications in appendix C.

2. Left-right model with spontaneous D-parity breaking

In this section we discuss the properties of left-right model with spontaneous D-parity breaking mechanism and state how it differs from the manifest left-right model.

2.1. Symmetric left-right model

The symmetric left-right model is based on the gauge group $SU(2)_L \times SU(2)_R \times U(1)_{B-L} \times SU(3)_C$ plus a discrete left-right parity symmetry. In these models, the discrete parity and $SU(2)_R$ gauge symmetry break simultaneously and thus the gauge couplings for $SU(2)_L$ and $SU(2)_R$ gauge groups remain equal i.e., $g_L = g_R$. The fermions and Higgs scalars are related in this model as,

$$\begin{aligned}
&\text{Fermions: } \psi_L \equiv \begin{pmatrix} \nu_L \\ \ell_L \end{pmatrix} \overset{P}{\Longleftrightarrow} \begin{pmatrix} \nu_R \\ \ell_R \end{pmatrix} \equiv \psi_R\,, \quad Q_L = \begin{pmatrix} u_R \\ d_R \end{pmatrix} \overset{P}{\Longleftrightarrow} Q_R = \begin{pmatrix} u_R \\ d_R \end{pmatrix} \\
&\text{Scalars: } \Delta_{L,R} \equiv \begin{pmatrix} \delta^+_{L,R}/\sqrt{2} & \delta^{++}_{L,R} \\ \delta^0_{L,R} & -\delta^+_{L,R}/\sqrt{2} \end{pmatrix} \quad \phi \equiv \begin{pmatrix} \phi^0_1 & \phi^+_2 \\ \phi^-_1 & \phi^0_2 \end{pmatrix}. \qquad (1)
\end{aligned}$$

The symmetry breaking of the left-right symmetric theory down to Standard Model and further to $G_{13} \equiv U(1)_Y \times SU(3)_C$ is achieved by the scalars $\Delta_{R,L}$ and Φ respectively. For a more detailed discussion on spontaneous symmetry breaking of left-right symmetry one may refer [39]. The vacuum expectation values (vev) of the scalars are given by,

$$\langle \Delta_{L,R} \rangle = \begin{pmatrix} 0 & 0 \\ v_{L,R} & 0 \end{pmatrix}, \quad \langle \Phi \rangle = \begin{pmatrix} k_1 & 0 \\ 0 & k_2 \end{pmatrix}$$

The invariant Yukawa Lagrangian under the symmetric left-right theory is

$$\begin{aligned}
\mathcal{L}_{\text{Yuk}} &= h_{ij}\overline{\nu}_L \langle \phi \rangle N_{jR} + \tilde{h}_{ij}\overline{\nu}_L \langle \tilde{\phi} \rangle N_{jR} + f_{ij}\left[N^T_{iR} C \langle \Delta_R \rangle N_{jR} + \nu^T_{iL} C \langle \Delta_L \rangle \nu_{jL}\right] + \text{h.c.} \\
&\subset h_{ij}\overline{\psi}_{iL}\phi\psi_{jR} + \tilde{h}_{ij}\overline{\psi}_{iL}\tilde{\phi}\psi_{jR} + f_{ij}\left[\psi^T_i C i\tau_2 \Delta_R \psi_{jR} + R \leftrightarrow L\right] + \text{h.c.} \qquad (2)
\end{aligned}$$

with $\tilde{\phi} \equiv \tau_2 \phi^* \tau_2$. The discrete left-right symmetry also results in equal Majorana couplings for left-handed and right-handed neutrinos. With these Yukawa terms the neutrino mass formula can be written as,

$$m_\nu = M_L - M_D \frac{1}{M_R} M_D^T = m_\nu^{II} + m_\nu^I \,, \tag{3}$$

where M_D is the Dirac neutrino mass matrix, $M_L = f\, v_L = f\, \langle \Delta_L \rangle_{\text{induced}}$ ($M_R = f\, v_R = f\, \langle \Delta_R \rangle$) is the Majorana mass term for left-handed (right-handed) neutrinos.

The seesaw relation in this case is found (from minimization of scalar potential consists of Φ, $\Delta_{L,R}$) to be,

$$v_L v_R = \gamma k^2 \,, \tag{4}$$

where $k = \sqrt{k_1^2 + k_2^2}$ and γ represents the function of various scalar coupling parameters in potential.

This means if one assign low mass to ν_L i.e. around eV scale, then ν_R has to lie at a very heavy scale, say 10^{13} to 10^{14} GeV which is well beyond the reach of current experiments. In order to bring down the right-handed scale to TeV, parity and $SU(2)_R$ have to be broken at TeV scale and also the Higgs couplings have to be finetuned to order of $\gamma \leq \mathcal{O}(10^{-10})$.

2.2. Asymmetric left-right model

Left-right theory with spontaneous D-parity breaking mechanism [62,63] is based on the idea that the discrete left-right symmetry (D parity) breaking scale and local $SU(2)_R$ breaking scale are decoupled from each other, i.e., D-parity breaks at an earlier stage as compared to $SU(2)_R$ gauge symmetry, thereby introducing a new scale. It should be noted here that, D-parity should not be confused with the Lorentz parity as latter one acts only on the fermionic content of the theory while D-parity interchanges the parity of the fermion as well as the $SU(2)_L \times SU(2)_R$ Higgs fields. It results in an asymmetric LR model for which the $SU(2)_L$ and $SU(2)_R$ gauge couplings become unequal i.e., $g_L \neq g_R$. This spontaneous breaking of D-parity occurs when singlet scalar σ takes vev which is odd under D-parity. The asymmetric left-right model then breaks down to SM symmetry with the help of right-handed triplet Higgs scalar Δ_R. Further SM symmetry breaks down to $U(1)_{\text{em}}$ theory with the help of scalar bidoublet Φ. The complete symmetry breaking can be sketched as follows,

- $SU(2)_L \times SU(2)_R \times U(1)_{B-L} \times SU(3)_C \times D \xrightarrow{\langle \sigma \rangle} SU(2)_L \times SU(2)_R \times U(1)_{B-L} \times SU(3)_C$
- $SU(2)_L \times SU(2)_R \times U(1)_{B-L} \times SU(3)_C \xrightarrow{\langle \Delta_R \rangle} SU(2)_L \times U(1)_Y \times SU(3)_C$
- $SU(2)_L \times U(1)_Y \times SU(3)_C \xrightarrow{\langle \Phi \rangle} U(1)_{\text{em}} \times SU(3)_C$

As $SU(2)_R$ breaking scale and parity breaking scale are different, there is no effect of left-handed scalar Δ_L at low energy and the fermion masses can be derived from the Yukawa Lagrangian. However, one can write an induced VEV for Δ_L from the seesaw relation as

$$v_L \approx \frac{\beta k^2 v_R}{2M M_P} \tag{5}$$

where M_P is D-parity breaking scale, β is a Higgs coupling constant of $\mathcal{O}(1)$ and $M \simeq M_P$.

This asymmetric left-right gauge theory can also emerge from high scale Pati-Salam theory having gauge group $SU(2)_L \times SU(2)_R \times SU(4)_C \times D$, i.e. $\mathcal{G}_{224D}$. Hence, we cite here two separate models implemented with spontaneous D-parity breaking mechanism, both having TeV scale asymmetric left-right model as an intermediate breaking step.

$$\begin{aligned} &\text{I. SO(10)} \xrightarrow{M_U} \mathcal{G}_{2213D} \xrightarrow{M_P} \mathcal{G}_{2213} \xrightarrow{M_R} G_{\rm SM} \xrightarrow{M_Z} G_{13} \\ &\text{II. SO(10)} \xrightarrow{M_U} \mathcal{G}_{224D} \xrightarrow{M_P} \mathcal{G}_{224} \xrightarrow{M_C} \mathcal{G}_{2213} \xrightarrow{M_R} G_{\rm SM} \xrightarrow{M_Z} G_{13} \end{aligned} \tag{6}$$

Here, M_U represents the unification scale (GUT scale), M_P, M_C, M_R and M_Z correspond to D-parity breaking, $SU(4)_C \to SU(3)_C \times U(1)_{B-L}$ breaking, LR-breaking and SM breaking scale respectively.

3. Neutrino masses and mixing via extended inverse seesaw mechanism

In manifest left-right symmetric models where neutrino mass is generated via type-I+type-II seesaw mechanism [49,50,53,54,57,70,71], one has to add either extra symmetry or do structural cancellation in order to align the right handed scale at TeV range. However the canonical seesaw contribution can be exactly canceled out in case of extended type-II seesaw [72] or inverse seesaw mechanism [73–75] and a large value of Dirac neutrino mass matrix, M_D can be obtained. These choices of seesaw allow large light-heavy neutrino mixing which facilitate rich phenomenology. However, generic inverse seesaw mechanism as proposed in ref. [76,77] gives negligible contribution to neutrinoless double beta decay as the associated sterile neutrino mass matrix μ_S lies in keV range to account for neutrino mass mechanism. Thus one has to extend the inverse seesaw mechanism with a large lepton number violating parameter in $N-N$ sector as M_N while keeping the same keV value of μ_S in the $S-S$ sector. Hence, the corresponding seesaw mechanism is termed as "extended inverse seesaw mechanism (EISS)" where the neutrino mass is governed by the standard inverse seesaw formula.

Henceforward we consider the model discussed in ref. [65] for our comparative study throughout the paper. In this model, gauged inverse seesaw mechanism is implemented by adding one extra fermion singlet S_i $(i = 1, 2, 3)$ per fermion generation. The extended seesaw mechanism is further gauged at TeV scale for which the VEV of the RH-doublet $\langle \chi_R^0 \rangle = v_\chi$ provides the $N-S$ mixing matrix M.

The asymmetric low-scale Yukawa Lagrangian can be written as,

$$\mathcal{L}_{\rm Yuk} = Y^\ell \overline{\ell}_L \, N_R \, \Phi + f \, N_R^c \, N_R \Delta_R + F \, \overline{N}_R \, S \, \chi_R + S^T \mu_S S + \text{h.c.} \tag{7}$$

which gives rise to the 9×9 neutral lepton mass matrix in the basis of $\begin{pmatrix} \nu_L & N_R & S \end{pmatrix}^T$ after electroweak symmetry breaking

$$\mathcal{M} = \begin{pmatrix} 0 & M_D & 0 \\ M_D^T & M_R & M^T \\ 0 & M & \mu_S \end{pmatrix}, \tag{8}$$

where $M_D = Y^\ell \langle \Phi \rangle$, $M_R = f \langle \Delta_R^0 \rangle$, $M = F \langle \chi_R^0 \rangle$. The Dirac neutrino mass matrix M_D is determined from the high scale symmetry and fits to charged fermion masses at GUT scale using RG evolution equations. In principle the $N-S$ mixing matrix M can assume any arbitrary form though we have taken it as diagonal. We have also treated the heavy RH Majorana neutrino mass

matrix M_R to be diagonal throughout this work. One essential outcome of extended inverse seesaw mechanism is that type-I seesaw contribution is exactly canceled out, type-II contribution is also damped out and thus inverse seesaw is the only viable contribution to light neutrino masses

$$m_\nu = \left(\frac{M_D}{M}\right) \mu_S \left(\frac{M_D}{M}\right)^T . \tag{9}$$

The heavy sterile neutrinos and heavy RH neutrinos with their mass matrices can be noted as, $M_S = \mu_S - M M_R^{-1} M^T$, $M_N = M_R + \cdots$.

As stated earlier, these block diagonal mass matrices m_ν, M_S and M_N can further be diagonalized to give physical masses to all neutral leptons by respective unitary mixing matrices: U_ν, U_S and U_N where

$$\begin{aligned} U_\nu^\dagger\, m_\nu\, U_\nu^* &= m_\nu^d = \text{diag}\left[m_{\nu_1}, m_{\nu_2}, m_{\nu_3}\right], \\ U_S^\dagger\, M_S\, U_S^* &= M_S^d = \text{diag}\left[M_{S_1}, M_{S_2}, M_{S_3}\right], \\ U_N^\dagger\, M_N\, U_N^* &= M_N^d = \text{diag}\left[M_{N_1}, M_{N_2}, M_{N_3}\right] \end{aligned} \tag{10}$$

The complete mixing matrix [65,78–80] diagonalizing the resulting 9×9 neutrino mass matrix turns out to be

$$\begin{aligned} \mathcal{V} &\equiv \begin{pmatrix} \mathcal{V}^{\nu\nu} & \mathcal{V}^{\nu S} & \mathcal{V}^{\nu N} \\ \mathcal{V}^{S\nu} & \mathcal{V}^{SS} & \mathcal{V}^{SN} \\ \mathcal{V}^{N\nu} & \mathcal{V}^{NS} & \mathcal{V}^{NN} \end{pmatrix} \\ &= \begin{pmatrix} \left(1 - \frac{1}{2} X X^\dagger\right) U_\nu & \left(X - \frac{1}{2} Z Y^\dagger\right) U_S & Z\, U_N \\ -X^\dagger\, U_\nu & \left(1 - \frac{1}{2}\{X^\dagger X + Y Y^\dagger\}\right) U_S & \left(Y - \frac{1}{2} X^\dagger Z\right) U_N \\ y^*\, X^\dagger\, U_\nu & -Y^\dagger\, U_S & \left(1 - \frac{1}{2} Y^\dagger Y\right)\, U_N \end{pmatrix} \end{aligned} \tag{11}$$

where the symbols are expressed in terms of model parameters as $X = M_D\, M^{-1}$, $Y = M\, M_N^{-1}$, $Z = M_D\, M_N^{-1}$, and $y = M^{-1}\, \mu_S$. With this mixing matrix, one can write the relevant charged current interactions of leptons valid at TeV scale asymmetric LR gauge theory (with $g_L \neq g_R$) in the flavor basis as

$$\mathcal{L}_{\text{CC}} = \frac{g}{\sqrt{2}} \sum_{\alpha = e,\mu,\tau} \left[\overline{\ell}_{\alpha\, L}\, \gamma_\mu\, \nu_{\alpha\, L}\, W_L^\mu + \overline{\ell}_{\alpha\, R}\, \gamma_\mu\, N_{\alpha\, R}\, W_R^\mu\right] + \text{h.c.}$$

The flavor eigenstates can be expressed in terms of mass eigenstates (ν_i, S_j, N_k) as

$$\begin{aligned} \nu_{\alpha\, L} &\sim \mathcal{V}_{\alpha\, i}^{\nu\nu}\, \nu_i + \mathcal{V}_{\alpha\, j}^{\nu\, S}\, S_j + \mathcal{V}_{\alpha\, k}^{\nu\, N}\, N_k\,, \\ N_{\alpha\, R} &\sim \mathcal{V}_{\alpha\, i}^{N\, \nu}\, \nu_i + \mathcal{V}_{\alpha\, j}^{N\, S}\, S_j + \mathcal{V}_{\alpha\, k}^{NN}\, N_k\,, \end{aligned} \tag{12}$$

where $i, j, k = 1, 2, 3$.

4. Numerical estimation of $0\nu\beta\beta$ contributions

We omit a detailed discussion on fermion mass fitting at GUT scale and derivation of M_D, M_N at TeV scale since this has been already done in ref. [65]. We simply use the derived model parameters of ref. [65] and extend the numerical estimation of non-standard contributions to $0\nu\beta\beta$ decay. Our major aim is to elucidate how unequal couplings i.e. $g_L \neq g_R$ enhance the rate of $0\nu\beta\beta$ transition in $W_R - W_R$ and $W_L - W_R$ channels.

Table 1
Different mass ranges of light active neutrinos ν_L, heavy RH neutrinos (N_R) and sterile neutrinos S_L for extended inverse seesaw (EISS) scheme.

EISS scheme	A	B	C
(M_1, M_2, M_3)	(30, 150, 2989) GeV	(100, 100, 4877) GeV	(50, 200, 1711) GeV
(M_{N1}, M_{N2}, M_{N3})	(500, 1000, 10000) GeV	(500, 5000, 10000) GeV	(1250, 3000, 5000) GeV
$m_{\nu 1}$	0.001268 eV	0.001268 eV	0.001269 eV
$m_{\nu 2}$	0.00879 eV	0.00879 eV	0.0088 eV
$m_{\nu 3}$	0.049 eV	0.049 eV	0.0492 eV
M_{S1}	1.8 GeV	1.99 GeV	1.9 GeV
M_{S2}	22.05 GeV	2.0 GeV	13.27 GeV
M_{S3}	827.87 GeV	2000 GeV	532 GeV

Here we present the numerical values of all the model parameters (Table 1). The Dirac neutrino mass matrix M_D derived at TeV scale (including RG corrections) has the form [65],

$$M_D = \begin{pmatrix} 0.02274 & 0.09891 - 0.01603i & 0.1462 - 0.3859i \\ 0.09891 + 0.01603i & 0.6319 & 4.884 + 0.0003034i \\ 0.1462 + 0.3859i & 4.884 - 0.0003034i & 117.8 \end{pmatrix} \text{GeV}. \quad (13)$$

The $N - S$ mixing matrix $M = \text{diag}[10.5, 120, 2500]$ GeV, and heavy RH neutrino mass matrix $M_N = \text{diag}[115, 1785, 7500]$ GeV provide mass eigenvalues to heavy sterile neutrinos $M_S = \text{diag}[1.06, 8.6, 887.6]$ GeV. As an immediate outcome, we get two mixing matrices for light-light neutrinos and light-sterile neutrinos as

$$\mathcal{V}^{\nu\nu} = \begin{pmatrix} 0.81494 + 0.00002\,i & 0.55801 - 0.000019\,i & -0.12659 - 0.091913\,i \\ -0.35953 - 0.049486\,i & 0.67140 - 0.03401\,i & 0.645155 + 0.00012\,i \\ 0.447078 - 0.057247\,i & -0.48392 - 0.03934\,i & 0.74554 - 0.000095\,i \end{pmatrix}, \quad (14)$$

$$\mathcal{V}^{\nu S} = \begin{pmatrix} 0.002165 & 0.00065 - 0.0001\,i & 0.00008 - 0.0002\,i \\ 0.0094 + 0.00152\,i & 0.0052 & 0.0019 + 1.16 \times 10^{-7}\,i \\ 0.0139 + 0.0367\,i & 0.0406 - 2.49 \times 10^{-6}\,i & 0.0457 \end{pmatrix}. \quad (15)$$

respectively.

Another key parameter is the mixing matrix for light and heavy RH Majorana neutrinos which is estimated to be

$$\mathcal{V}^{\nu N} = \begin{pmatrix} 0.000198 & 0.000055 - 8.980 \times 10^{-6}\,i & 0.000019 - 0.0000514\,i \\ 0.00086 + 0.00014\,i & 0.000354 & 0.00065 + 4. \times 10^{-8}\,i \\ 0.0012768 + 0.00337\,i & 0.002736 - 1.68 \times 10^{-7}\,i & 0.0157 \end{pmatrix}. \quad (16)$$

$$\mathcal{V}^{N\nu} = \begin{pmatrix} 0.00113266 - 0.0017284\,i & 0.00145509 - 0.00195787\,i & 0.00171826 - 0.00288543\,i \\ 0.00149292 + 7.97906 \times 10^{-6}\,i & 0.00174197 + 5.26889 \times 10^{-6}\,i & 0.00244734 + 1.45034 \times 10^{-6}\,i \\ 0.00781003 + 0.0000451934\,i & 0.0088384 + 0.0000296147\,i & 0.0130124 + 7.49586 \times 10^{-6}\,i \end{pmatrix}. \quad (17)$$

Also the mixing matrix between heavy RH Majorana neutrinos and light-sterile neutrinos can be estimated as,

Table 2
Range of g_R for different breaking chains.

Breaking chain	g_R	g_L	$\delta = \frac{g_R}{g_L}$
Case I	0.632	0.632	1
Case II	0.589	0.632	0.93
Case IIIA	0.39	0.632	0.62
Case IIIB	0.414	0.632	0.65

$$\mathcal{V}^{NN} = \text{diag}[0.995832, 0.99774, 0.94444] \tag{18}$$

$$\mathcal{V}^{NS} = \text{diag}[-0.0913043, -0.0672269, -0.33333] \tag{19}$$

Here we focus only on those scenarios where mass of neutrinos is either small or greater than the typical momentum exchange scale in $0\nu\beta\beta$ transition i.e. $\langle p^2 \rangle \simeq 190\,\text{MeV}^2$. The estimated effective mass parameter for standard contribution is found to be 0.0044 eV for NH (Normal Hierarchy), 0.048 eV for IH (Inverted Hierarchy) and 0.35 eV for QD (Quasi Degenerate) nature of light neutrinos while the bound provided by KamLAND-Zen experiment is 0.23 eV. A stringent limit on sum of the light neutrino masses by Planck collaboration i.e. $\sum_{i=1}^{3} m_{\nu_i} \lesssim 0.23$ constraints the QD nature of light neutrinos while other hierarchical nature of light neutrinos can not be probed at present. Hence, one should explore possible new physics contributions in order to saturate the recent $0\nu\beta\beta$ experimental bound. We numerically estimate how the half-lives of the isotopes is enhanced due to different new contributions arising in the model and present a comparative study of the same in symmetric and asymmetric case.

Using the values of M_D, M, M_N and the corresponding mixing between light active neutrinos ν_L, heavy RH neutrinos (N_R) and sterile neutrinos S along with other known parameters, the model predictions for different LNV dimensionless parameters and their experimental limits are presented in Table 6. In order to estimate these LNV parameters, we have fixed $M_{W_L} = 83.187$ GeV, $M_{W_R} \gtrsim 3.1$ TeV [81–84], $g_R \simeq 0.39 - 0.632$, $g_L \simeq 0.632$, $m_e = 0.51$ MeV and $m_p = 935$ MeV. The limits on these LNV parameters have been derived from the recent KamLAND-ZEN experiment [22].

For the four different cases (as discussed in Appendix C) the range for g_R is tabulated in Table 2. However, for the calculations in the rest of the paper we consider three cases I, II and III since for case IIIA and IIIB the values of $\delta = \frac{g_R}{g_L}$ are nearly equal.

5. Comparative study of $0\nu\beta\beta$ contributions with D-parity breaking mechanism

Predictions on neutrinoless double beta decay in LR model with Spontaneous D-parity breaking and half-life with proper nuclear matrix element and normalized lepton number violating effective mass parameters have been discussed in the appendix section. In this section we present a comparative study of different contributions to neutrinoless double beta decay process arising due to mediation of either one W_R^- or two W_R^- gauge bosons in terms of half-life and effective mass parameters within the frameworks of symmetric and asymmetric left-right model. In an asymmetric left-right model, when we express non-standard contributions for $0\nu\beta\beta$ via $W_R - W_R$ and $W_L - W_R$ channels which involves $SU(2)_R$ gauge coupling transitions in terms of known parameters like Fermi coupling constant G_F^2 then these expressions carry a overall factor like $\frac{g_R}{g_L}$ in Feynman amplitudes and $\frac{g_L}{g_R}$ in half-life estimation. Depending upon the value of g_L, g_R

Table 3
Effective mass parameters for the present asymmetric TeV scale LR model with spontaneous D-parity breaking where $SU(2)_R$ and discrete parity breaks at different scale and its comparison with those quantities in symmetric LR model.

Effective mass parameter (symmetric LR model)	Effective mass parameter (asymmetric LR model (Case II))	Suppression factor m_{ee}^{D}/m_{ee}
$\mathbf{m}_{ee}^{\nu} = 0.0044\,\text{eV}$	$\mathbf{m}_{ee}^{\nu,D} = 0.0044\,\text{eV}$	1
$\mathbf{m}_{ee,L}^{S} = 104.93\,\text{eV}$	$\mathbf{m}_{ee,L}^{S,D} = 104.93\,\text{eV}$	1
$\mathbf{m}_{ee,L}^{N} = 0.0033\,\text{eV}$	$\mathbf{m}_{ee,L}^{N,D} = 0.0033\,\text{eV}$	1
$\mathbf{m}_{ee,R}^{N} = 0.040\,\text{eV}$	$\mathbf{m}_{ee,R}^{N,D} = 0.030\,\text{eV}$	$\left(\frac{g_R}{g_L}\right)^4 \simeq 0.75$
$\mathbf{m}_{ee}^{\Delta_R} = 1.74 \times 10^{-20}\,\text{eV}$	$\mathbf{m}_{ee}^{\Delta_R,D} = 1.30 \times 10^{-20}\,\text{eV}$	$\left(\frac{g_R}{g_L}\right)^4 \simeq 0.75$
$\mathbf{m}_{ee}^{\lambda,\nu} = 1.142\,\text{eV}$	$\mathbf{m}_{ee}^{\lambda,\nu,D} = 0.988\,\text{eV}$	$\left(\frac{g_R}{g_L}\right)^2 \simeq 0.86$
$\mathbf{m}_{ee}^{\lambda,S} = 0.0035\,\text{eV}$	$\mathbf{m}_{ee}^{\lambda,S,D} = 0.0030\,\text{eV}$	$\left(\frac{g_R}{g_L}\right)^2 \simeq 0.86$
$\mathbf{m}_{ee}^{\lambda,N} = 4.486 \times 10^{-8}\,\text{eV}$	$\mathbf{m}_{ee}^{\lambda,S,D} = 3.858 \times 10^{-8}\,\text{eV}$	$\left(\frac{g_R}{g_L}\right)^2 \simeq 0.86$
$\mathbf{m}_{ee}^{\eta} = 2.16\,\text{eV}$	$\mathbf{m}_{ee}^{\eta,D} = 2.16\,\text{eV}$	1

Table 4
Effective mass parameters for the present asymmetric TeV scale LR model with spontaneous D-parity breaking (after introducing Pati-Salam symmetry) where $SU(2)_R$ and discrete parity breaks at different scale and its comparison with those quantities in symmetric LR model.

Effective mass parameter (symmetric LR model)	Effective mass parameter (asymmetric LR model (Case III))	Suppression factor m_{ee}^{D}/m_{ee}
$\mathbf{m}_{ee}^{\nu} = 0.0044\,\text{eV}$	$\mathbf{m}_{ee}^{\nu,D} = 0.0044\,\text{eV}$	1
$\mathbf{m}_{ee,L}^{S} = 104.93\,\text{eV}$	$\mathbf{m}_{ee,L}^{S,D} = 104.93\,\text{eV}$	1
$\mathbf{m}_{ee,L}^{N} = 0.0033\,\text{eV}$	$\mathbf{m}_{ee,L}^{N,D} = 0.0033\,\text{eV}$	1
$\mathbf{m}_{ee,R}^{N} = 0.040\,\text{eV}$	$\mathbf{m}_{ee,R}^{N,D} = 0.0052\,\text{eV}$	$\left(\frac{g_R}{g_L}\right)^4 \simeq 0.13$
$\mathbf{m}_{ee}^{\Delta_R} = 1.74 \times 10^{-20}\,\text{eV}$	$\mathbf{m}_{ee}^{\Delta_R,D} = 2.58 \times 10^{-21}\,\text{eV}$	$\left(\frac{g_R}{g_L}\right)^4 \simeq 0.13$
$\mathbf{m}_{ee}^{\lambda,\nu} = 1.142\,\text{eV}$	$\mathbf{m}_{ee}^{\lambda,\nu,D} = 0.411\,\text{eV}$	$\left(\frac{g_R}{g_L}\right)^2 \simeq 0.36$
$\mathbf{m}_{ee}^{\lambda,S} = 0.0035\,\text{eV}$	$\mathbf{m}_{ee}^{\lambda,S,D} = 0.0013\,\text{eV}$	$\left(\frac{g_R}{g_L}\right)^2 \simeq 0.37$
$\mathbf{m}_{ee}^{\lambda,N} = 4.486 \times 10^{-8}\,\text{eV}$	$\mathbf{m}_{ee}^{\lambda,S,D} = 1.615 \times 10^{-8}\,\text{eV}$	$\left(\frac{g_R}{g_L}\right)^2 \simeq 0.36$
$\mathbf{m}_{ee}^{\eta} = 2.16\,\text{eV}$	$\mathbf{m}_{ee}^{\eta,D} = 2.16\,\text{eV}$	1

and the ratio $\frac{g_R}{g_L}$, there are different contributions which are either suppressed or enhanced as compared to the $0\nu\beta\beta$ transition derived in a symmetric left-right theory.

We have presented the numerical estimation of effective mass parameters comparing the symmetric (case-I) as well as asymmetric (case-II) LR model (without introducing Pati Salam symmetry) in Table 3. For a non-SUSY $SO(10)$ GUT where Pati-Salam symmetry with D-parity occurs as the highest intermediate symmetry breaking step, the RG evolution of gauge couplings predicts $g_L = 0.65$ and $g_R = 0.39$ at TeV scale. This particular set up gives the ratio $\left(\frac{g_R}{g_L}\right) = 0.6$. The numerical values of effective mass parameter in symmetric and asymmetric cases are compared in Table 4. Estimated value of half-life for $0\nu\beta\beta$ transition due to different

Table 5
Estimated value of half-life for $0\nu\beta\beta$ transition due to different nuclei and corresponding experimental limits.

Nucleus	Model prediction for $T_{1/2}^{0\nu}$ (yrs)	Current limits	Future limits
^{76}Ge	1.3×10^{25}-4.13×10^{27}	$\gtrsim 8.0 \times 10^{25}$ yrs	$\gtrsim 6.0 \times 10^{27}$ yrs
^{136}Xe	1.03×10^{25}-6.13×10^{27}	$\gtrsim 1.6 \times 10^{26}$ yrs	$\gtrsim 8.0 \times 10^{27}$ yrs

Table 6
Estimated values of lepton number violating (LNV) parameters within the framework of TeV scale asymmetric left-right model with $g_L \neq g_R$.

LNV parameters	Estimated value (Case I)	Estimated value (Case II)	Estimated value (Case III)	Experimental limit
η_ν	8.73×10^{-9}	8.73×10^{-9}	8.73×10^{-9}	$\lesssim 2.66 \times 10^{-7}$
$\eta_{LL}^{S,N}$	2.45×10^{-10}	2.45×10^{-10}	2.45×10^{-10}	$\lesssim 2.55 \times 10^{-9}$
η_{RR}^{ν}	1.932×10^{-19}	1.445×10^{-19}	2.50×10^{-20}	$\lesssim 2.66 \times 10^{-7}$
$\eta_{RR}^{S,N}$	1.09×10^{-9}	8.154×10^{-10}	1.41×10^{-10}	$\lesssim 2.55 \times 10^{-9}$
$\eta_{RR}^{\Delta_R}$	1.63×10^{-11}	1.22×10^{-11}	2.41×10^{-12}	$\lesssim 2.55 \times 10^{-9}$
η_η	2.65×10^{-9}	2.65×10^{-9}	2.65×10^{-9}	$\lesssim 1.13 \times 10^{-9}$
η_λ	1.51×10^{-7}	1.31×10^{-7}	5.43×10^{-8}	$\lesssim 2.18 \times 10^{-7}$

nuclei and their current experimental bounds as well as future sensitivity have been tabulated in Table 5. The suppression factor in effective mass parameters is found to be $\left(\frac{g_R}{g_L}\right)^4 \simeq 0.13$ in the $W_R - W_R$ channel via exchange of heavy RH neutrinos and heavy RH Higgs triplets while in the $W_L - W_R$ channel it is found to be $\left(\frac{g_R}{g_L}\right)^2 \simeq 0.36$. Similarly, new contributions involving right-handed charged current interaction are enhanced and the enhancement factor is found to be $\left(\frac{g_L}{g_R}\right)^8 \simeq 59.29$ in the $W_R - W_R$ channel via exchange of heavy RH neutrinos and RH Higgs triplets while it is $\left(\frac{g_L}{g_R}\right)^2 \simeq 7.7$ in the $W_L - W_R$ channel. The same is shown in Table 8. If we do not introduce the Pati Salam symmetry in the unification scenario, we will get negligible enhancement of half-life estimation for asymmetric LR model as compared to symmetric one. The result of such estimation has been tabulated in Table 7.

6. Results and conclusion

One important outcome of extended inverse seesaw scheme is that type-I seesaw contribution is exactly canceled out thereby allowing the possibility of large left-right mixing in the neutrino sector. The occurrence of Pati-Salam symmetry at the highest scale gives large value to Dirac neutrino mass matrix M_D and thus the mixed helicity λ and η diagrams contribute dominantly to the $0\nu\beta\beta$ transition. At the same time, the $W_R - W_R$ mediated diagrams due to exchange of heavy RH neutrinos also deliver dominant contributions to the process. In addition, another important contribution comes from purely left-handed currents via $W_L - W_L$ mediation due to

Table 7
Expression for half-lives governing $0\nu\beta\beta$ transition in TeV scale symmetric and asymmetric left-right models. $\left[\mathbf{T}^{0\nu}_{1/2}\right]_D$ stands for half-life expression in case of a LR model with spontaneous D-parity breaking while $\left[\mathbf{T}^{0\nu}_{1/2}\right]$ stands for half-life expression in symmetric LR model.

Half-life (Case I)	Half-life (Case II)	Enhancement factor $\left[T^{0\nu}_{1/2}\right]_D / \left[T^{0\nu}_{1/2}\right]$
$\left[\mathbf{T}^{0\nu}_{1/2}\right]_N = \mathbf{1}/\left(\mathcal{K}_{0\nu}\lvert\mathbf{m}^N_{ee}\rvert^2\right)$	$\left[\mathbf{T}^{0\nu}_{1/2}\right]_{N,D} = \mathbf{1}/\left(\mathcal{K}_{0\nu}\lvert\mathbf{m}^N_{ee,D}\rvert^2\right)$	$\left(\frac{g_L}{g_R}\right)^8 \simeq 1.78$
$\left[\mathbf{T}^{0\nu}_{1/2}\right]_{\Delta_R} = \mathbf{1}/\left(\mathcal{K}_{0\nu}\lvert\mathbf{m}^{\Delta_R}_{ee}\rvert^2\right)$	$\left[\mathbf{T}^{0\nu}_{1/2}\right]_{\Delta_R,D} = \mathbf{1}/\left(\mathcal{K}_{0\nu}\lvert\mathbf{m}^{\Delta_R}_{ee,D}\rvert^2\right)$	$\left(\frac{g_L}{g_R}\right)^8 \simeq 1.78$
$\left[\mathbf{T}^{0\nu}_{1/2}\right]_{\lambda} = \mathbf{1}/\left(\mathcal{K}_{0\nu}\lvert\mathbf{m}^{\lambda}_{ee}\rvert^2\right)$	$\left[\mathbf{T}^{0\nu}_{1/2}\right]_{\lambda,D} = \mathbf{1}/\left(\mathcal{K}_{0\nu}\lvert\mathbf{m}^{\lambda}_{ee,D}\rvert^2\right)$	$\left(\frac{g_L}{g_R}\right)^4 \simeq 1.33$

Table 8
Expression for half-lives governing $0\nu\beta\beta$ transition in symmetric and asymmetric left-right models. Case-I is for symmetric left-right model ($g_L = g_R$), Case-III is where D-parity breaking in Pati-Salam symmetry leads to $g_L \neq g_R$.

Half-life (Case I)	Half-life (Case III)	Enhancement factor $\left[T^{0\nu}_{1/2}\right]_D / \left[T^{0\nu}_{1/2}\right]$
$\left[\mathbf{T}^{0\nu}_{1/2}\right]_N = \mathbf{1}/\left(\mathcal{K}_{0\nu}\lvert\mathbf{m}^N_{ee}\rvert^2\right)$	$\left[\mathbf{T}^{0\nu}_{1/2}\right]_{N,D} = \mathbf{1}/\left(\mathcal{K}_{0\nu}\lvert\mathbf{m}^N_{ee,D}\rvert^2\right)$	$\left(\frac{g_L}{g_R}\right)^8 \simeq 59.29$
$\left[\mathbf{T}^{0\nu}_{1/2}\right]_{\Delta_R} = \mathbf{1}/\left(\mathcal{K}_{0\nu}\lvert\mathbf{m}^{\Delta_R}_{ee}\rvert^2\right)$	$\left[\mathbf{T}^{0\nu}_{1/2}\right]_{\Delta_R,D} = \mathbf{1}/\left(\mathcal{K}_{0\nu}\lvert\mathbf{m}^{\Delta_R}_{ee,D}\rvert^2\right)$	$\left(\frac{g_L}{g_R}\right)^8 \simeq 59.29$
$\left[\mathbf{T}^{0\nu}_{1/2}\right]_{\lambda} = \mathbf{1}/\left(\mathcal{K}_{0\nu}\lvert\mathbf{m}^{\lambda}_{ee}\rvert^2\right)$	$\left[\mathbf{T}^{0\nu}_{1/2}\right]_{\lambda,D} = \mathbf{1}/\left(\mathcal{K}_{0\nu}\lvert\mathbf{m}^{\lambda}_{ee,D}\rvert^2\right)$	$\left(\frac{g_L}{g_R}\right)^4 \simeq 7.7$

exchange of heavy sterile neutrinos. We have also discussed that LR model with spontaneous D-parity breaking mechanism gives different analytic expressions for different $0\nu\beta\beta$ contributions in the $W_R - W_R$ and $W_L - W_R$ mediated channels since the theory predicts unequal gauge couplings for $SU(2)_L$ and $SU(2)_R$ gauge groups. We have embedded the model in non-supersymmetric $SO(10)$ GUT and discussed different symmetry breaking chains, i.e. with and without Pati-Salam symmetry for showing how the enhancement factor $\left(\frac{g_L}{g_R}\right)$ for half-life prediction of neutrinoless double beta decay changes for different cases. When Pati-Salam symmetry is not included in the symmetry breaking chain, we get the enhancement factor $\left(\frac{g_L}{g_R}\right)^8 \simeq 1.78$ for $W_R - W_R$ channel while for the $W_L - W_R$ channel the enhancement factor is $\left(\frac{g_L}{g_R}\right)^4 \simeq 1.33$. However the enhancement factor increases significantly when Pati-Salam symmetry appears in the symmetry breaking chain. In this case, the enhancement factor becomes $\left(\frac{g_L}{g_R}\right)^8 \simeq 59.29$ for $W_R - W_R$ channel and for $W_L - W_R$ channel the enhancement factor becomes $\left(\frac{g_L}{g_R}\right)^4 \simeq 7.7$. Pati-Salam symmetry also plays an important role in predicting values of $SU(2)_L$ and $SU(2)_R$ gauge couplings for which we get the values; $g_L = 0.632$ and $g_R \simeq 0.39$.

We have shown various plots to infer how half-life of $0\nu\beta\beta$ decay due to different channels varies with the ratio $\frac{g_R}{g_L}$ i.e. δ and mass of W_R. From Fig. 1 we see that the cyan shaded region

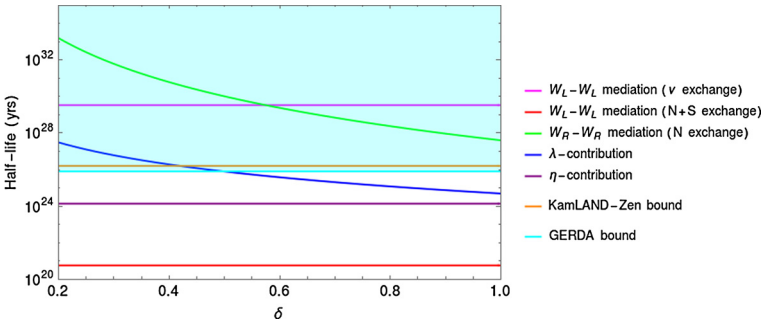

Fig. 1. Half life of $0\nu\beta\beta$ process due to all possible channels in the model vs δ ($= \frac{g_R}{g_L}$). The orange horizontal line represents recent KamLAND-Zen bound while the blue line represents GERDA bound on half life of the process. The cyan shaded region shows the allowed range for half life. (For interpretation of the colors in the figure(s), the reader is referred to the web version of this article.)

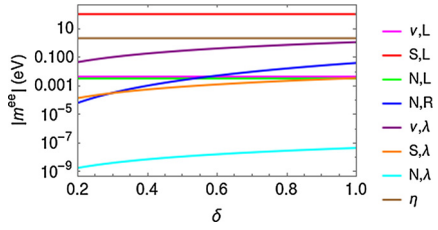

Fig. 2. The plot shows how effective Majorana mass parameter due to different decay channels varies with δ.

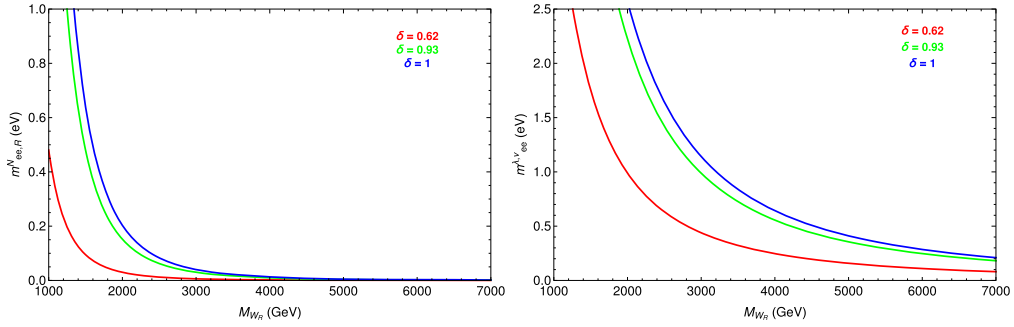

Fig. 3. The plot in the left panel shows effective Majorana mass parameter due to heavy neutrino, N exchange in purely right-handed currents vs W_R mass, where W_R mass varies from 1 to 3 TeV. The plot in the right panel shows effective Majorana mass parameter due to $W_L - W_R$ mixing (λ diagram) with ν exchange vs W_R mass. In both the plots three different values of δ are considered: δ=0.63, 0.93, 1.

is sensitive to the current KamLAND-Zen and GERDA bounds. Since the value of the ratio $\frac{g_R}{g_L}$ ranges from 0.62 to 1 for three different cases considered in the work, the plot shows only the contributions from $W_L - W_L$ channel due to light neutrino exchange and from $W_R - W_R$ channel due to heavy neutrino exchange lie within the privileged region. Fig. 2 shows how the effective Majorana mass parameter varies with the ratio δ. Only non-trivial M_{W_R} dependence occurs for the contribution arise from $W_R - W_R$ mediation with RH neutrino exchange as well as from $W_L - W_R$ mediation (λ-contribution). So, Fig. 3 shows how the effective Majorana mass

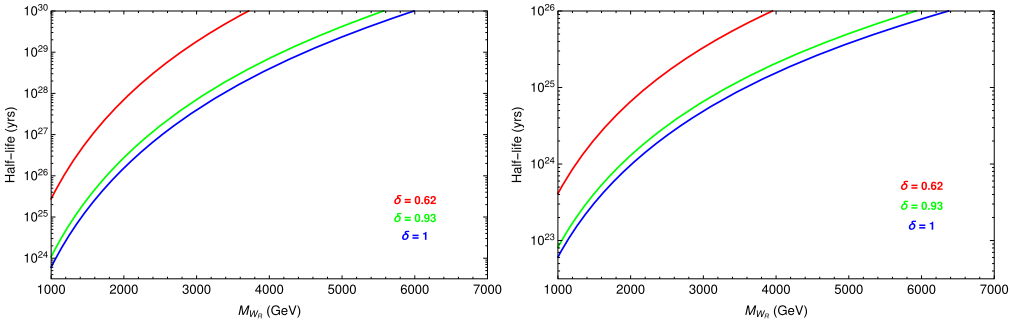

Fig. 4. Plot in the left panel shows half life due to N exchange in $W_R - W_R$ channel vs mass of W_R while plot in the right panel shows half life due to all λ diagrams (ν, N, S exchange with $W_L - W_R$ mixing) vs mass of W_R. In both the plots three different values of δ are considered: δ=0.63, 0.93, 1.

parameter due to these two decay channels vary with the mass of W_R and the variation of half life with W_R mass has been presented in Fig. 4. For Fig. 3 and 4, the mass range for W_R has been considered here as, $M_{W_R} \in [1, 7]$ TeV for better transparency.

Declaration of competing interest

The authors declare that they have no known competing financial interests or personal relationships that could have appeared to influence the work reported in this paper.

Acknowledgements

SS is thankful to UGC for fellowship grant to support her research work. The authors thank Prof. Urjit A. Yajnik for useful comments and discussion.

Appendix A. Predictions on neutrinoless double beta decay in LR model with spontaneous D-parity breaking

The importance of neutrinoless double beta decay process in particle physics is far-reaching in the sense that it is one such process which can confirm the Majorana nature of neutrino and also provide information about the absolute scale of light neutrino mass. Neutrinoless Double Beta Decay can be induced by the exchange of a light Majorana neutrino, which is called the standard mechanism or by some other lepton number violating physics which is called the non-standard interpretation [39,77,79,85–94]. In the standard mechanism the parent nucleus emits a pair of virtual W bosons, and then these exchange a Majorana neutrino to produce the outgoing electrons. At the vertex where it is emitted, the exchanged neutrino is created, in association with an electron, as an antineutrino with almost total positive helicity, and only its small, $O(m_\nu/E)$, negative-helicity component is absorbed at the other vertex. In LRSM the process can be mediated by heavy right-handed neutrino and some new channels can also appear due to left-right mixing, i.e. $W_L - W_R$ mixing. In the considered model many diagrams are possible due to the presence of heavy neutrinos S, N, doubly charged Higgs scalar Δ_R and $W_L - W_R$ mixing. We will discuss that in this section, but we start by writing the charged current interaction Lagrangian for the model in flavor basis.

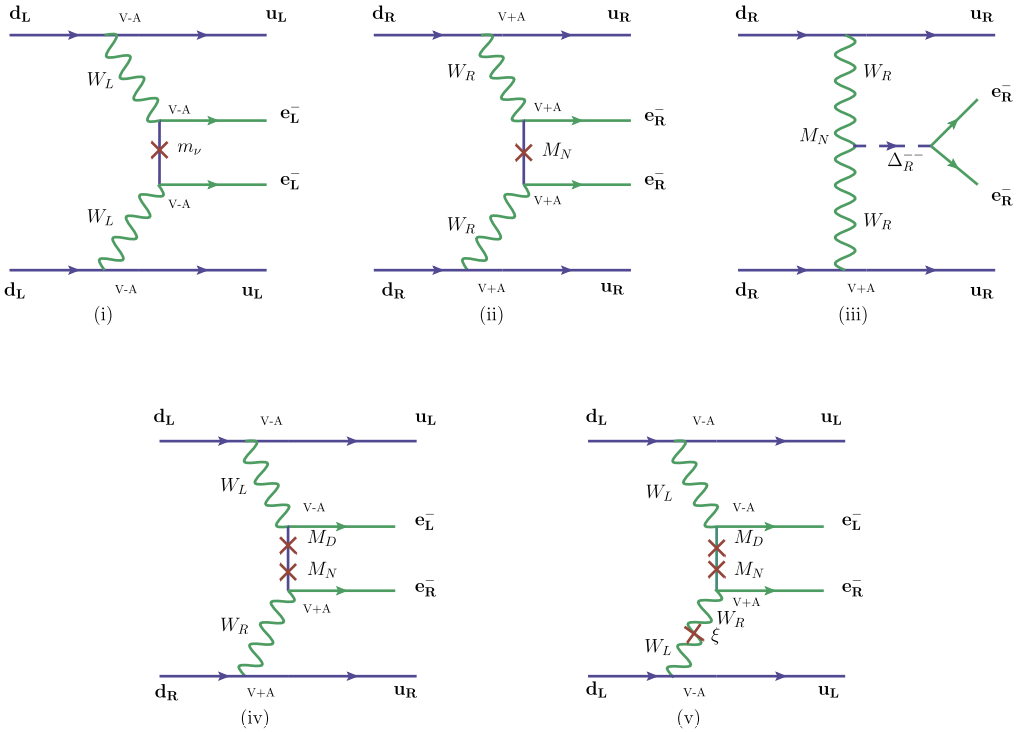

Fig. 5. Relevant Feynman diagrams contributing to neutrinoless double decay process within the framework of left-right symmetric models.

$$
\begin{aligned}
\mathcal{L}_{\rm CC} &= \frac{g_L}{\sqrt{2}} \sum_{\alpha=e,\mu,\tau} \overline{\ell}_{\alpha\, L}\, \gamma_\mu \nu_{\alpha\, L}\, W_L^\mu + \frac{g_R}{\sqrt{2}} \sum_{\alpha=e,\mu,\tau} \overline{\ell}_{\alpha\, R}\, \gamma_\mu N_{\alpha\, R}\, W_R^\mu + \text{h.c.} \\
&= \frac{g_L}{\sqrt{2}}\, \overline{e}_{L}\, \gamma_\mu \nu_{e\, L}\, W_L^\mu + \frac{g_R}{\sqrt{2}}\, \overline{e}_{R}\, \gamma_\mu N_{e\, R}\, W_R^\mu + \text{h.c.} \quad \text{only for first generation} \\
&= \frac{g_L}{\sqrt{2}} \left[\overline{e}_{L}\, \gamma_\mu \{ \mathcal{V}_{e\,i}^{\nu\nu}\, \nu_i + \mathcal{V}_{e\,i}^{\nu\, S}\, S_i + \mathcal{V}_{e\,i}^{\nu\, N}\, N_i \}\, W_L^\mu \right] + \text{h.c.} \\
&\quad + \frac{g_R}{\sqrt{2}} \left[\overline{e}_{R}\, \gamma_\mu \{ \mathcal{V}_{\alpha\,i}^{N\,\nu}\, \nu_i + \mathcal{V}_{\alpha\,i}^{N\,S}\, S_i + \mathcal{V}_{\alpha\,i}^{NN}\, N_i \}\, W_R^\mu \right] + \text{h.c.}
\end{aligned}
\tag{A.1}
$$

Since we have considered that the left-handed and right-handed charged gauge bosons mix with each other the physical gauge bosons can be expressed as linear combinations of W_L and W_R as,

$$
\begin{cases}
W_1 = \quad \cos\xi\ W_L + \sin\xi\ W_R \\
W_2 = -\sin\xi\ W_L + \cos\xi\ W_R
\end{cases}
\tag{A.2}
$$

with mixing angle ξ, we have

$$
|\tan 2\xi| \sim \frac{k_1\, k_2}{v_R^2} \sim \frac{k_2}{k_1} \frac{g_{\rm R}^2}{g_{\rm L}^2} \left(\frac{M_{W_L}^2}{M_{W_R}^2} \right) \leq 10^{-4}. \tag{A.3}
$$

Different types of Feynman diagrams contributing to the $0\nu\beta\beta$ process are [65] shown in Fig. 5.

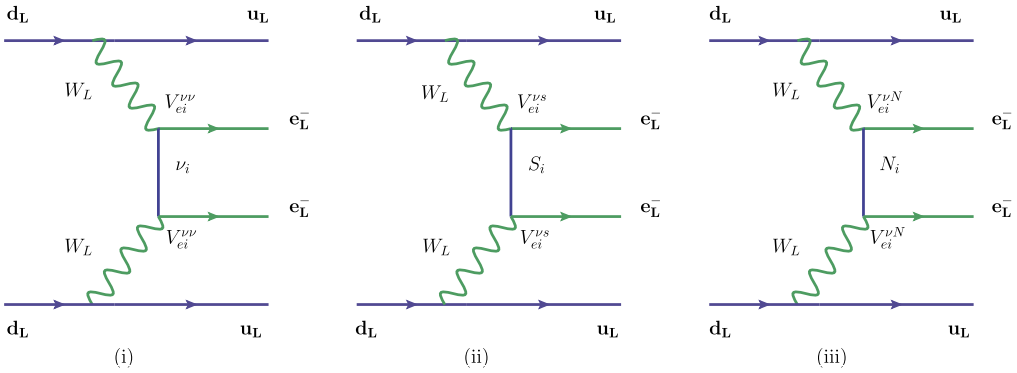

Fig. 6. Relevant Feyman Diagrams due to $W_L^- - W_L^-$ channel.

(i) Feynman diagrams in $W_L^- - W_L^-$ channel (with two left-handed currents)
(ii) Feynman diagrams in $W_R^- - W_R^-$ channel (with two right-handed currents)
(iii) Doubly charged Higgs scalar exchange with right-handed currents (this can also be possible with left-handed currents)
(iv) Neutrino and W_R exchanges with Dirac mass helicity flip in $W_L - W_R$ channel (λ mechanism)
(v) Neutrino and W_L exchanges with Dirac mass helicity flip and $W_L - W_R$ mixing in the $W_L - W_R$ channel (η mechanism)

A.1. Mass-dependent mechanisms due to $W_L^- - W_L^-$ channel and $W_R^- - W_R^-$ channel

Now, let's write the amplitudes for these processes and the corresponding particle physics parameter involving lepton number violation. The Feynman amplitude for the processes having both left-handed electrons is proportional to

$$\mathcal{A}_{LL} \simeq G_F^2 \left(1 + 2\tan\xi + \tan^2\xi\right) \sum_i \left(\frac{\mathcal{V}_{ei}^{\nu\nu 2} m_i}{p^2} - \frac{\mathcal{V}_{ei}^{\nu S 2}}{M_{S_i}} - \frac{\mathcal{V}_{ei}^{\nu N 2}}{M_{N_i}} \right), \tag{A.4}$$

where, m_i, M_{S_i}, and M_{N_i} are the masses of light neutrino ν and heavy neutrinos S and N respectively and $\tan\xi$ represents left-right gauge boson mixing. The diagrams are separately shown in Fig. 6.

Similarly, the Feynman amplitudes for the processes involving $W_R^- - W_R^-$ mediation via exchanges of either light or heavy neutrinos where both the emitted electrons are right-handed is proportional to,

$$\mathcal{A}_{RR} \simeq G_F^2 \left[\left(\frac{M_{W_L}}{M_{W_R}}\right)^4 \left(\frac{g_R}{g_L}\right)^4 + 2\left(\frac{M_{W_L}}{M_{W_R}}\right)^2 \left(\frac{g_R}{g_L}\right)^2 \tan\xi + \tan^2\xi \right] \times \sum_i \left(\frac{\mathcal{V}_{ei}^{\nu N 2} m_i}{p^2} - \frac{\mathcal{V}_{ei}^{NS 2}}{M_{S_i}} - \frac{\mathcal{V}_{ei}^{NN 2}}{M_{N_i}} \right). \tag{A.5}$$

The suitably normalized dimensionless parameters that describe lepton number violation are

$$
\begin{aligned}
|\eta^{\nu}_{LL}| &= \left| \frac{\sum_i \mathcal{N}^2_{ei} m_i}{m_e} \right| \quad , \quad |\eta^{\nu}_{RR}| = \left(\frac{g_R}{g_L}\right)^4 \left| \left(\frac{M_{W_L}}{M_{W_R}}\right)^4 \frac{\sum_i \mathcal{V}^{N\nu 2}_{ei} m_i}{m_e} \right| , \\
|\eta^{S}_{LL}| &= \left| -m_p \frac{\sum_i \mathcal{V}^{\nu S 2}_{ei}}{M_{S_i}} \right| \quad , \quad |\eta^{S}_{RR}| = \left(\frac{g_R}{g_L}\right)^4 \left| -\left(\frac{M_{W_L}}{M_{W_R}}\right)^4 m_p \frac{\sum_i \mathcal{V}^{NS 2}_{ei}}{M_{S_i}} \right| , \\
|\eta^{N}_{LL}| &= \left| -m_p \frac{\sum_i \mathcal{V}^{\nu N 2}_{ei}}{M_{N_i}} \right| \quad , \quad |\eta^{N}_{RR}| = \left(\frac{g_R}{g_L}\right)^4 \left| -\left(\frac{M_{W_L}}{M_{W_R}}\right)^4 m_p \frac{\sum_i \mathcal{V}^{NN 2}_{ei}}{M_{N_i}} \right| .
\end{aligned}
\tag{A.6}
$$

A.2. Triplet exchange mechanisms

Fig. 5 (iii) is mediated by $SU(2)_R$ scalar triplet Δ_R and for this the amplitude is given by

$$
\mathcal{A}_{\Delta_R} \simeq G_F^2 \left(\frac{M_{W_L}}{M_{W_R}}\right)^4 \left(\frac{g_R}{g_L}\right)^4 \sum_i \frac{V^2_{ei} M_i}{m^2_{\Delta^{--}_R}} \propto \frac{L^4}{R^5} , \tag{A.7}
$$

and the dimensionless particle physics parameter is

$$
\left|\eta^{\Delta_R}_{RR}\right| = \left(\frac{M_{W_L}}{M_{W_R}}\right)^4 \left(\frac{g_R}{g_L}\right)^4 \frac{m_p \left|\sum_i V^2_{ei} M_i\right|}{m^2_{\Delta^{--}_R}} . \tag{A.8}
$$

A.3. Momentum dependent mechanisms

In this case the emitted electrons have opposite helicity, and the amplitude is proportional to

$$
\begin{aligned}
\mathcal{A}_{LR} \simeq\ & G_F^2 \left(\left(\frac{M_{W_L}}{M_{W_R}}\right)^2 \left(\frac{g_R}{g_L}\right)^2 + \tan\xi + \left(\frac{M_{W_L}}{M_{W_R}}\right)^2 \left(\frac{g_R}{g_L}\right)^2 \tan\xi + \tan^2\xi \right) \\
& \times \sum_i \left(\mathcal{V}^{\nu\nu}_{ei} \mathcal{V}^{N\nu *}_{ei} \frac{1}{|p|} - \mathcal{V}^{\nu S}_{ei} \mathcal{V}^{NS *}_{ei} \frac{|p|}{M^2_{S_i}} - \mathcal{V}^{\nu N}_{ei} \mathcal{V}^{NN *}_{ei} \frac{|p|}{M^2_{N_i}} \right) ;
\end{aligned}
\tag{A.9}
$$

and corresponding dimensionless particle physics parameter involving lepton number violation are

$$
\begin{aligned}
|\eta_{\lambda,\nu}| &= \left(\frac{g_R}{g_L}\right)^2 \left| \left(\frac{M_{W_L}}{M_{W_R}}\right)^2 \sum_i \mathcal{N}_{ei} \mathcal{V}^{N\nu *}_{ei} \right| , \qquad |\eta_{\eta,\nu}| = \left| \tan\xi \sum_i \mathcal{N}_{ei} \mathcal{V}^{N\nu *}_{ei} \right| , \\
|\eta_{\lambda,S}| &= \left(\frac{g_R}{g_L}\right)^2 \left| \left(\frac{M_{W_L}}{M_{W_R}}\right)^2 \sum_i \mathcal{V}^{\nu S}_{ei} \mathcal{V}^{NS *}_{ei} \frac{|p|^2}{M^2_{S_i}} \right| , \quad |\eta_{\eta,S}| = \left| \tan\xi \sum_i \mathcal{V}^{\nu S}_{ei} \mathcal{V}^{NS *}_{ei} \frac{|p|^2}{M^2_{S_i}} \right| , \\
|\eta_{\lambda,N}| &= \left(\frac{g_R}{g_L}\right)^2 \left| \left(\frac{M_{W_L}}{M_{W_R}}\right)^2 \sum_i \mathcal{V}^{\nu N}_{ei} \mathcal{V}^{NN *}_{ei} \frac{|p|^2}{M^2_{N_i}} \right| , \quad |\eta_{\eta,N}| = \left| \tan\xi \sum_i \mathcal{V}^{\nu N}_{ei} \mathcal{V}^{NN *}_{ei} \frac{|p|^2}{M^2_{N_i}} \right| ,
\end{aligned}
\tag{A.10}
$$

Appendix B. Life time with proper nuclear matrix element and normalized effective mass parameters

We express the inverse half-life in terms of effective mass parameters with proper normalization factors taking into account the nuclear matrix elements [49,95,96] leading to the half-life prediction

$$[T^{0\nu}_{1/2}]^{-1} = G^{0\nu}_{01}\Big\{|\mathcal{M}^{0\nu}_{\nu}|^2|\eta^{\rm light}_{LL}|^2 + |\mathcal{M}^{0\nu}_{N}|^2|\eta^{\rm heavy}_{LL}|^2 + |\mathcal{M}^{0\nu}_{\nu}|^2|\eta^{\rm light}_{RR}|^2 + |\mathcal{M}^{0\nu}_{N}|^2|\eta^{\rm heavy}_{RR}|^2 + |\mathcal{M}^{0\nu}_{\lambda}\eta_{\lambda} + \mathcal{M}^{0\nu}_{\eta}\eta_{\eta}|^2\Big\}. \tag{B.1}$$

$G^{0\nu}_{01}$ is the phase space factor and matrix elements are $\mathcal{M}^{0\nu}_{k}$ $(k = \nu, N, \lambda, \eta)$. Also the dimensionless LNV particle physics parameters are

$$|\eta_{\nu}| = \frac{1}{m_e}\left|\sum_{i=1}^{3}\mathcal{V}^{\nu\nu 2}_{ei}m_{\nu_i}\right| \lesssim 2.66\times 10^{-7}, \tag{B.2}$$

$$|\eta^{\rm heavy}_{LL}| = m_p\left|-\sum_{i=1}^{3}\frac{\mathcal{V}^{\nu S2}_{ei}}{M_{S_i}} - \sum_{i=1}^{3}\frac{\mathcal{V}^{\nu N2}_{ei}}{M_{N_i}}\right| \lesssim 2.55\times 10^{-9}, \tag{B.3}$$

$$|\eta^{\rm light}_{RR}| = \frac{1}{m_e}\left(\frac{M_{W_L}}{M_{W_R}}\right)^4\left(\frac{g_R}{g_L}\right)^4\left|\sum_{i=1}^{3}\mathcal{V}^{N\nu 2}_{ei}m_{\nu_i}\right| \lesssim 2.66\times 10^{-7}, \tag{B.4}$$

$$|\eta^{\rm heavy}_{RR}| = m_p\left(\frac{M_{W_L}}{M_{W_R}}\right)^4\left(\frac{g_R}{g_L}\right)^4\left|-\sum_{i=1}^{3}\frac{\mathcal{V}^{\nu S2}_{ei}}{M_{S_i}} - \sum_{i=1}^{3}\frac{\mathcal{V}^{NN2}_{ei}}{M_{N_i}}\right| \lesssim 2.55\times 10^{-9}, \tag{B.5}$$

$$|\eta_{\lambda}| = \left(\frac{M_{W_L}}{M_{W_R}}\right)^2\left(\frac{g_R}{g_L}\right)^2\left|\sum_{i=1}^{3}\mathcal{V}^{\nu N}_{ei}\mathcal{V}^{NN}_{ei}\right| \lesssim 2.18\times 10^{-7}, \tag{B.6}$$

$$|\eta_{\eta}| = \tan\xi\left|\sum_{i=1}^{3}\mathcal{V}^{\nu N}_{ei}\mathcal{V}^{NN}_{ei}\right| \lesssim 1.13\times 10^{-9}, \tag{B.7}$$

where, m_e (m_i)= mass of electron (light neutrino), and m_p = mass of proton. Besides different particle physics parameters, it contains the nuclear matrix elements due to different chiralities of the hadronic weak currents such as $\left(\mathcal{M}^{0\nu}_{\nu}\right)$ involving left-left chirality in the standard contribution, and $\left(\mathcal{M}^{0\nu}_{\nu}\right)$ involving right-right chirality arising out of heavy neutrino exchange, $\left(\mathcal{M}^{0\nu}_{\lambda}\right)$ for the λ diagram, and $\left(\mathcal{M}^{0\nu}_{\eta}\right)$ for the η diagram. It is to be noted here that the current bound on these LNV parameters are derived based on half-life limit from the KamLAND-Zen experiment neglecting interference terms.

The numerical values of these nuclear matrix elements as discussed in ref. [49,95,96] are given in Table 9.

Using the expression for inverse half-life of $0\nu\beta\beta$ decay process due to only light neutrinos, $\left[T^{0\nu}_{1/2}\right]^{-1} = G^{0\nu}_{01}\left|\mathcal{M}^{0\nu}_{\nu}\right|^2|\eta_{\nu}|^2$, we can arrive at a suitable normalization factor for all types of

Table 9
Phase space factors and nuclear matrix elements with their allowed ranges.

Isotope	$G_{01}^{0\nu}$	$\mathcal{M}_{\nu}^{0\nu}$	$\mathcal{M}_{N}^{0\nu}$	$\mathcal{M}_{\lambda}^{0\nu}$	$\mathcal{M}_{\eta}^{0\nu}$
^{76}Ge	5.77×10^{-15}	2.58–6.64	233–412	1.75–3.76	235–637
^{136}Xe	3.56×10^{-14}	1.57–3.85	164–172	1.92–2.49	370–419

contributions. Using the numerical values given in Table 9, we rewrite the inverse half-life in terms of effective mass parameter as,

$$\left[T_{1/2}^{0\nu}\right]^{-1} = G_{01}^{0\nu}\left|\frac{\mathcal{M}_{\nu}^{0\nu}}{m_e}\right|^2 |\mathbf{m}_{\rm ee}^{\nu}|^2 = 1.57\times 10^{-25}\,\mathrm{yrs}^{-1}\,\mathrm{eV}^{-2}|\mathbf{m}_{\rm ee}^{\nu}|^2 = \mathcal{K}_{0\nu}\,|\mathbf{m}_{\rm ee}^{\nu}|^2$$

where $\mathbf{m}_{\rm ee}^{\nu} = \sum_i \left(\mathcal{V}_{ei}^{\nu\nu}\right)^2 m_{\nu_i}$. Then the analytic expression for all other contributions taking into account the respective nuclear matrix elements turns out to be

$$\begin{aligned}\left[T_{1/2}^{0\nu}\right]^{-1} &= \mathcal{K}_{0\nu}\left[|\mathbf{m}_{\rm ee}^{\nu}|^2 + |\mathbf{m}_{\rm ee,L}^{S,N}|^2 + |\mathbf{m}_{\rm ee,R}^{S,N}|^2 + |\mathbf{m}_{\rm ee}^{\lambda}|^2 + |\mathbf{m}_{\rm ee}^{\eta}|^2\right] + \cdots \\ &= \mathcal{K}_{0\nu}\Big[|\mathbf{m}_{\rm ee}^{\nu}|^2 + |\mathbf{m}_{\rm ee,L}^{S} + \mathbf{m}_{\rm ee,L}^{N}|^2 + |\mathbf{m}_{\rm ee,R}^{S} + \mathbf{m}_{\rm ee,R}^{N}|^2 \\ &\quad + |\mathbf{m}_{\rm ee}^{\lambda,\nu} + \mathbf{m}_{\rm ee}^{\lambda,S} + \mathbf{m}_{\rm ee}^{\lambda,N}|^2 + |\mathbf{m}_{\rm ee}^{\eta,\nu} + \mathbf{m}_{\rm ee}^{\eta,S} + \mathbf{m}_{\rm ee}^{\eta,N}|^2\Big] + \cdots \end{aligned} \tag{B.8}$$

where the ellipses denote interference terms and all other subdominant contributions. Also the individual effective LNV parameters can be expressed as

$$\mathbf{m}_{\nu}^{\rm ee} = \sum_{i=1}^{3} \mathcal{V}_{ei}^{\nu\nu 2}\, m_{\nu_i} \tag{B.9}$$

$$\mathbf{m}_{\rm ee,L}^{S} = \sum_{i=1}^{3} \mathcal{V}_{ei}^{\nu S 2}\,\frac{|p|^2}{M_{S_i}} \tag{B.10}$$

$$\mathbf{m}_{\rm ee,L}^{N} = \sum_{i=1}^{3} \mathcal{V}_{ei}^{\nu N 2}\,\frac{|p|^2}{M_{N_i}} \tag{B.11}$$

$$\mathbf{m}_{\rm ee,R}^{N} = \sum_{i=1}^{3} \left(\frac{m_{W_L}}{m_{W_R}}\right)^4 \left(\frac{g_R}{g_L}\right)^4 \mathcal{V}_{ei}^{NN 2}\,\frac{|p|^2}{M_{N_i}} \tag{B.12}$$

$$\mathbf{m}_{\rm ee}^{\lambda,\nu} = 10^{-2}\left(\frac{M_{W_L}}{M_{W_R}}\right)^2 \left(\frac{g_R}{g_L}\right)^2 |p| \sum_{i=1}^{3}\left[U_{\rm PMNS}\frac{M_D}{M_N}\cdots\right]_{ee} \tag{B.13}$$

$$\mathbf{m}_{\rm ee}^{\lambda,S} = 10^{-2}\left(\frac{m_{W_L}}{m_{W_R}}\right)^2 \left(\frac{g_R}{g_L}\right)^2 \sum_{i=1}^{3} \mathcal{V}_{ei}^{\nu S}\mathcal{V}^{NS}\,\frac{|p|^3}{M_{S_i}^2} \tag{B.14}$$

$$\mathbf{m}_{\rm ee}^{\lambda,N} = 10^{-2}\left(\frac{m_{W_L}}{m_{W_R}}\right)^2 \left(\frac{g_R}{g_L}\right)^2 \sum_{i=1}^{3} \mathcal{V}_{ei}^{\nu N}\mathcal{V}^{NN}\,\frac{|p|^3}{M_{N_i}^2} \tag{B.15}$$

$$\mathbf{m}_{\rm ee}^{\eta} = \tan\zeta_{LR}\,|p|\sum_{i=1}^{3}\left[U_{\rm PMNS}\frac{M_D}{M_N}\cdots\right]_{ee} \tag{B.16}$$

where $\langle p\rangle^2 = -m_e\, m_p\, \mathcal{M}_N^{0\nu}/\mathcal{M}_\nu^{0\nu} \simeq |200\ \text{MeV}|^2$. It is to be noted that the suppression factor 10^{-2} arises in the λ diagram because of normalization w.r.t. the standard mechanism.

Appendix C. The role of Pati-Salam symmetry

We know that both the gauge couplings for $SU(2)_L$ and $SU(2)_R$ are exactly equal at a scale when either Pati-Salam symmetry with discrete left-right symmetry $SU(2)_L \times SU(2)_R \times SU(4)_C \times D \equiv \mathcal{G}_{224D}$ or manifest left-right symmetry $SU(2)_L \times SU(2)_R \times U(1)_{B-L} \times SU(3)_C \times D \equiv \mathcal{G}_{2213D}$ appears as an intermediate symmetry breaking step. This equality is sustained as long as D-parity remains unbroken. Once the spontaneous breaking of D-parity occurs, it immediately results in $g_L \neq g_R$ and the ratio $\frac{g_L}{g_R}$ deviates from unity depending upon the breaking scale. In the considered model we have found this ratio $\frac{g_L}{g_R}$ to be $\simeq 1.5$ which will be supportive in predicting new non-standard contributions to neutrinoless double beta decay. The deviation of this ratio from unity is enhanced by the occurrence of Pati-Salam symmetry as an intermediate scale and thus justifies its importance in explaining $0\nu\beta\beta$, LFV decays as well as collider processes within the framework of $SO(10)$ GUT based models. The importance of Pati-Salam symmetry as the highest intermediate step in a SO(10) symmetry breaking chain has already been discussed in ref. [68]. For quantifying these points, we consider the following non-SUSY $SO(10)$ chain, as an example.

$$SO(10) \xrightarrow{M_U} \mathcal{G}_{224D} \xrightarrow{M_P} \mathcal{G}_{224} \xrightarrow{M_C} \mathcal{G}_{2213} \xrightarrow{M_R} \mathcal{G}_{SM} \xrightarrow{M_Z} \mathcal{G}_{13}\,.$$

It was found that the G_{224}-singlets contained in $\{54\}_H$ and $\{210\}_H$ of $SO(10)$ are D-parity even and odd, respectively. Moreover the neutral components of the G_{224} multiplet $\{1,1,15\}$ contained in $\{210\}_H$ and $\{45\}_H$ of $SO(10)$ were also found to be D-parity even and odd, respectively. Here in the first step, VEV is assigned to the $\langle(1,1,1)\rangle \subset \{54\}_H$ which has even D-Parity to ensure the survival of LR symmetric Pati-Salam group while in the second step D-parity is broken by assigning $\langle(1,1,1)\rangle \subset \{210\}_H$ to obtain asymmetric G_{224} with $g_L \neq g_R$. Then the spontaneous breaking of $G_{224} \to G_{2213}$ is achieved by the VEV $\langle(1,1,15)_H^0\rangle \subset \{210\}_H$. The breaking of $SU(2)_R \times U(1)_{B-L} \to U(1)_Y$ is achieved by $\langle\Delta_R^0\rangle \subset \{126\}_H$ while the VEV $\langle\chi_R^0\rangle \subset \{16\}_H$ provides the N-S mixing. Finally, as usual, the breaking of SM to low energy theory $U(1)_{\rm em} \times SU(3)_C$ is carried out by the SM bidoublet $\Phi \subset \{10\}_H$.

C.1. Gauge coupling unification

We consider three different cases for gauge coupling unification as follows and we also show the Higgs spectrum used in different ranges of mass scales under respective gauge symmetries.

Case - I: Symmetric LR model ($g_L = g_R$)

$$SO(10) \xrightarrow{M_U} \mathcal{G}_{2213D} \xrightarrow{M_R} \mathcal{G}_{SM} \xrightarrow{M_Z} \mathcal{G}_{13}\,.$$

(i) $\mu = \mathbf{M_Z} - \mathbf{M_R} : \mathcal{G} = \text{SM} = \mathcal{G}_{213},\quad \phi(2,1/2,1)\,;$

(ii) $\mu = \mathbf{M_R} - \mathbf{M_U} : \mathcal{G} = \mathcal{G}_{2213},\quad \Phi_1(2,2,0,1) \oplus \Phi_2(2,2,0,1) \oplus \chi_L(2,1,-1,1) \oplus$
$\chi_R(1,2,-1,1) \oplus \Delta_L(3,1,2,1) \oplus \Delta_R(1,3,2,1) \oplus$

$$4\delta^{+}(1,1,2,1) \oplus \eta(1,1,-2/3,3) \oplus \xi(1,1,4/3,6) \tag{C.1}$$

Case - II: Asymmetric LR model ($g_L \neq g_R$)

$$SO(10) \xrightarrow{M_U} \mathcal{G}_{2213D} \xrightarrow{M_C} \mathcal{G}_{2213} \xrightarrow{M_R} \mathcal{G}_{SM} \xrightarrow{M_Z} \mathcal{G}_{13}\,.$$

$$\begin{aligned}
&\text{(i)}\,\mu = \mathbf{M_Z} - \mathbf{M_R} : \mathcal{G} = \text{SM} = \mathcal{G}_{213}, \quad \phi(2,1/2,1)\,; \\
&\text{(ii)}\,\mu = \mathbf{M_R} - \mathbf{M_U} : \mathcal{G} = \mathcal{G}_{2213}, \quad \Phi_1(2,2,0,1) \oplus \Phi_2(2,2,0,1) \oplus \chi_R(1,2,-1,1) \oplus \\
&\qquad\qquad \Delta_R(1,3,2,1) \oplus 6\delta^{+}(1,1,2,1)
\end{aligned} \tag{C.2}$$

Now, we have introduced the Pati-Salam symmetry in the $SO(10)$ symmetry breaking chain. We have divided case-III into IIIA and IIIB where IIIA stands for the case where $SO(10)$ and D-parity break at same scale ($M_U \approx M_P$) and in IIIB, we have presented the D-parity breaking at some lower scale than M_U.

Case - IIIA:

$$SO(10) \xrightarrow{M_U \approx M_P} \mathcal{G}_{224} \xrightarrow{M_C} \mathcal{G}_{2213} \xrightarrow{M_R} \mathcal{G}_{SM} \xrightarrow{M_Z} \mathcal{G}_{13}\,.$$

$$\begin{aligned}
&\text{(i)}\,\mu = \mathbf{M_Z} - \mathbf{M_R} : \mathcal{G} = \text{SM} = \mathcal{G}_{213}, \quad \phi(2,1/2,1)\,; \\
&\text{(ii)}\,\mu = \mathbf{M_R} - \mathbf{M_C} : \mathcal{G} = \mathcal{G}_{2213}, \quad \Phi_1(2,2,0,1) \oplus \Phi_2(2,2,0,1) \oplus \chi_L(2,1,-1,1) \oplus \\
&\qquad\qquad \chi_R(1,2,-1,1) \oplus \Delta_L(3,1,-2,1) \oplus \Delta_R(1,3,-2,1)\,; \\
&\text{(iii)}\,\mu = \mathbf{M_C} - \mathbf{M_U} : \mathcal{G} = \mathcal{G}_{224}, \quad \Phi_1(2,2,1) \oplus \Phi_2(2,2,1) \oplus \chi_R(1,2,\bar{4}) \oplus \\
&\qquad\qquad \Delta_R(1,3,\bar{10}) \oplus \Omega_R(1,3,15) \oplus \Sigma(1,1,15) \oplus \\
&\qquad\qquad \zeta(2,2,15) \oplus \eta(2,2,1) \oplus \rho(2,1,4)\,.
\end{aligned} \tag{C.3}$$

Case - IIIB:

$$SO(10) \xrightarrow{M_U} \mathcal{G}_{224D} \xrightarrow{M_P} \mathcal{G}_{224} \xrightarrow{M_C} \mathcal{G}_{2213} \xrightarrow{M_R} \mathcal{G}_{SM} \xrightarrow{M_Z} \mathcal{G}_{13}\,.$$

$$\begin{aligned}
&\text{(i)}\,\mu = \mathbf{M_Z} - \mathbf{M_R} : \mathcal{G} = \text{SM} = \mathcal{G}_{213}, \quad \phi(2,1/2,1)\,; \\
&\text{(ii)}\,\mu = \mathbf{M_R} - \mathbf{M_C} : \mathcal{G} = \mathcal{G}_{2213}, \quad \Phi_1(2,2,0,1) \oplus \Phi_2(2,2,0,1) \oplus \chi_L(2,1,-1,1) \oplus \\
&\qquad\qquad \chi_R(1,2,-1,1) \oplus \Delta_L(3,1,-2,1) \oplus \Delta_R(1,3,-2,1)\,; \\
&\text{(iii)}\,\mu = \mathbf{M_C} - \mathbf{M_P} : \mathcal{G} = \mathcal{G}_{224}, \quad \Phi_1(2,2,1) \oplus \Phi_2(2,2,1) \oplus \chi_R(1,2,\bar{4}) \oplus \\
&\qquad\qquad \Delta_R(1,3,\bar{10}) \oplus \Omega_R(1,3,15) \oplus \\
&\qquad\qquad \Sigma(1,1,15) \oplus \xi(2,2,15)\,; \\
&\text{(iv)}\,\mu = \mathbf{M_P} - \mathbf{M_U} : \mathcal{G} = \mathcal{G}_{224D}, \quad \Phi_1(2,2,1) \oplus \Phi_2(2,2,1) \oplus \chi_L(2,1,4) \oplus \\
&\qquad\qquad \chi_R(1,2,\bar{4}) \oplus \Delta_L(3,1,10) \oplus \Delta_R(1,3,\bar{10}) \oplus \\
&\qquad\qquad \Omega_L(3,1,15) \oplus \Omega_R(1,3,15) \oplus \\
&\qquad\qquad \Sigma(1,1,15) \oplus \xi(2,2,15) \;\oplus \sigma(1,1,1)\,.
\end{aligned} \tag{C.4}$$

The gauge coupling unification plots for the above four cases are shown in Fig. 7 and Fig. 8 respectively. In the unification plots the different colored lines stand for running of various gauge groups. The red, blue, pink, magenta and green lines are for $SU(2)_L$, $SU(2)_R$, $U(1)_Y$, $U(1)_{B-L}$, $SU(3)_C$ gauge groups respectively. For case-IIIB we have added an extra particle $\xi(2,2,15)$

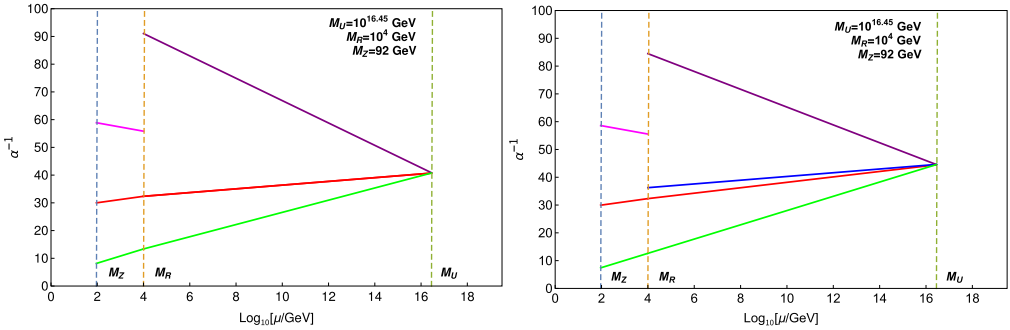

Fig. 7. The plot in the left panel shows gauge coupling unification at the scale $M_U = 10^{16.45}$ GeV for the symmetric LRSM case, i.e. $g_L = g_R$ (case-I). The plot in the right panel shows gauge coupling unification at the scale $M_U = 10^{16.45}$ GeV for the asymmetric LRSM case, i.e. $g_L \neq g_R$ without Pati-Salam symmetry (case-II).

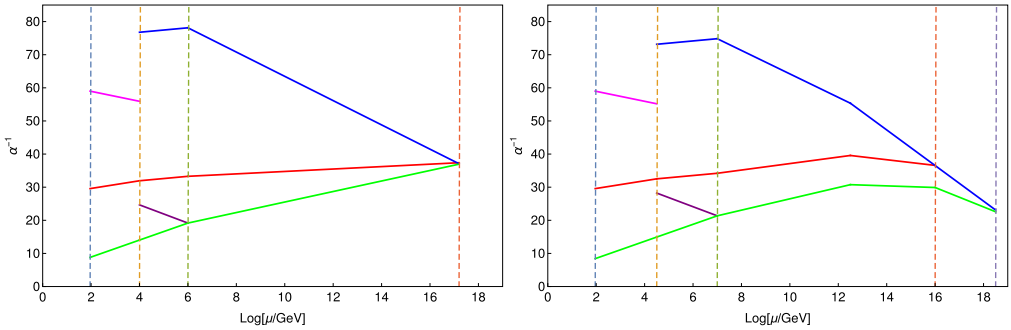

Fig. 8. The left panel plot shows the gauge coupling unification as well as D-parity breaking at $M_U \sim M_P = 10^{17.2}$ GeV (Case-IIIA). In the right panel, we present the unification at about $M_U = 10^{18.5}$ GeV after introducing Pati-Salam symmetry as the highest intermediate symmetry breaking scale with D-parity breaking at around $M_P = 10^{16}$ GeV (Case-IIIB). For both the cases, $g_L \neq g_R$.

which helps us to unify the $SU(2)_L$ and $SU(2)_R$ gauge couplings at around 10^{16} GeV (i.e., the D-parity breaking scale of $\mathcal{G}_{224D}$), also this extension of the model gives us the advantage to acquire fermion mass fitting at GUT scale.

References

[1] Super-Kamiokande Collaboration, S. Fukuda, et al., Constraints on neutrino oscillations using 1258 days of Super-Kamiokande solar neutrino data, Phys. Rev. Lett. 86 (2001) 5656–5660, arXiv:hep-ex/0103033.
[2] SNO Collaboration, Q.R. Ahmad, et al., Direct evidence for neutrino flavor transformation from neutral current interactions in the Sudbury Neutrino Observatory, Phys. Rev. Lett. 89 (2002) 011301, arXiv:nucl-ex/0204008.
[3] SNO Collaboration, Q.R. Ahmad, et al., Measurement of day and night neutrino energy spectra at SNO and constraints on neutrino mixing parameters, Phys. Rev. Lett. 89 (2002) 011302, arXiv:nucl-ex/0204009.
[4] J.N. Bahcall, C. Pena-Garay, Solar models and solar neutrino oscillations, New J. Phys. 6 (2004) 63, arXiv:hep-ph/0404061.
[5] T2K Collaboration, K. Abe, et al., Indication of electron neutrino appearance from an accelerator-produced off-axis muon neutrino beam, Phys. Rev. Lett. 107 (2011) 041801, arXiv:1106.2822.
[6] MINOS Collaboration, P. Adamson, et al., Improved search for muon-neutrino to electron-neutrino oscillations in MINOS, Phys. Rev. Lett. 107 (2011) 181802, arXiv:1108.0015.
[7] Double Chooz Collaboration, Y. Abe, et al., Indication of reactor $\bar{\nu}_e$ disappearance in the Double Chooz experiment, Phys. Rev. Lett. 108 (2012) 131801, arXiv:1112.6353.

[8] RENO Collaboration, J.K. Ahn, et al., Observation of reactor electron antineutrino disappearance in the RENO experiment, Phys. Rev. Lett. 108 (2012) 191802, arXiv:1204.0626.
[9] Daya Bay Collaboration, F.P. An, et al., Observation of electron-antineutrino disappearance at Daya Bay, Phys. Rev. Lett. 108 (2012) 171803, arXiv:1203.1669.
[10] P. Minkowski, $\mu \to e\gamma$ at a rate of one out of 10^9 muon decays?, Phys. Lett. B 67 (1977) 421–428.
[11] T. Yanagida, Horizontal gauge symmetry and masses of neutrinos, Conf. Proc. C7902131 (1979) 95–99.
[12] M. Gell-Mann, P. Ramond, R. Slansky, Complex spinors and unified theories, Conf. Proc. C790927 (1979) 315–321, arXiv:1306.4669.
[13] R.N. Mohapatra, G. Senjanovic, Neutrino mass and spontaneous parity nonconservation, Phys. Rev. Lett. 44 (1980) 912, 231 (1979).
[14] T.P. Cheng, L.-F. Li, Neutrino masses, mixings and oscillations in SU(2) × U(1) models of electroweak interactions, Phys. Rev. D 22 (1980) 2860.
[15] G. Lazarides, Q. Shafi, C. Wetterich, Proton lifetime and fermion masses in an SO(10) model, Nucl. Phys. B 181 (1981) 287–300.
[16] M. Magg, C. Wetterich, Neutrino mass problem and gauge hierarchy, Phys. Lett. B 94 (1980) 61–64.
[17] J. Schechter, J.W.F. Valle, Neutrino masses in SU(2) × U(1) theories, Phys. Rev. D 22 (1980) 2227.
[18] R. Foot, H. Lew, X.G. He, G.C. Joshi, Seesaw neutrino masses induced by a triplet of leptons, Z. Phys. C 44 (1989) 441.
[19] E. Ma, Pathways to naturally small neutrino masses, Phys. Rev. Lett. 81 (1998) 1171–1174, arXiv:hep-ph/9805219.
[20] E. Majorana, Teoria simmetrica dell'elettrone e del positrone, Nuovo Cimento 14 (1937) 171–184.
[21] J. Schechter, J.W.F. Valle, Neutrinoless double beta decay in SU(2) × U(1) theories, Phys. Rev. D 25 (1982) 2951, 289 (1981).
[22] KamLAND-Zen Collaboration, H. Ozaki, A. Takeuchi, Upgrade of the KamLAND-Zen mini-balloon and future prospects, Nucl. Instrum. Methods Phys. Res., Sect. A (2019) 162353.
[23] GERDA Collaboration, M. Agostini, et al., Upgrade for Phase II of the Gerda experiment, Eur. Phys. J. C 78 (5) (2018) 388, arXiv:1711.01452.
[24] Planck Collaboration, N. Aghanim, et al., Planck 2018 results. VI. Cosmological parameters, arXiv:1807.06209.
[25] S. Vagnozzi, E. Giusarma, O. Mena, K. Freese, M. Gerbino, S. Ho, M. Lattanzi, Unveiling ν secrets with cosmological data: neutrino masses and mass hierarchy, Phys. Rev. D 96 (12) (2017) 123503, arXiv:1701.08172.
[26] E. Giusarma, S. Vagnozzi, S. Ho, S. Ferraro, K. Freese, R. Kamen-Rubio, K.-B. Luk, Scale-dependent galaxy bias, CMB lensing-galaxy cross-correlation, and neutrino masses, Phys. Rev. D 98 (12) (2018) 123526, arXiv:1802.08694.
[27] E. Giusarma, M. Gerbino, O. Mena, S. Vagnozzi, S. Ho, K. Freese, Improvement of cosmological neutrino mass bounds, Phys. Rev. D 94 (8) (2016) 083522, arXiv:1605.04320.
[28] Particle Data Group Collaboration, M. Tanabashi, et al., Review of particle physics, Phys. Rev. D 98 (3) (2018) 030001.
[29] KATRIN Collaboration, M. Aker, et al., Improved upper limit on the neutrino mass from a direct kinematic method by KATRIN, Phys. Rev. Lett. 123 (22) (2019) 221802, arXiv:1909.06048.
[30] KATRIN Collaboration, A. Osipowicz, et al., KATRIN: a next generation tritium beta decay experiment with sub-eV sensitivity for the electron neutrino mass. Letter of intent, arXiv:hep-ex/0109033.
[31] KATRIN Collaboration, J. Angrik, et al., KATRIN design report 2004 (2005).
[32] KATRIN Collaboration, M. Arenz, et al., First transmission of electrons and ions through the KATRIN beamline, J. Instrum. 13 (04) (2018) P04020, arXiv:1802.04167.
[33] M. Kleesiek, et al., β-decay spectrum, response function and statistical model for neutrino mass measurements with the KATRIN experiment, Eur. Phys. J. C 79 (3) (2019) 204, arXiv:1806.00369.
[34] R.N. Mohapatra, J.C. Pati, A natural left-right symmetry, Phys. Rev. D 11 (1975) 2558.
[35] J.C. Pati, A. Salam, Lepton number as the fourth color, Phys. Rev. D 10 (1974) 275–289, Erratum: Phys. Rev. D 11 (1975) 703.
[36] G. Senjanovic, R.N. Mohapatra, Exact left-right symmetry and spontaneous violation of parity, Phys. Rev. D 12 (1975) 1502.
[37] G. Senjanovic, Spontaneous breakdown of parity in a class of gauge theories, Nucl. Phys. B 153 (1979) 334–364.
[38] R.N. Mohapatra, G. Senjanovic, Neutrino masses and mixings in gauge models with spontaneous parity violation, Phys. Rev. D 23 (1981) 165.
[39] P. Pritimita, N. Dash, S. Patra, Neutrinoless double beta decay in LRSM with natural type-II seesaw dominance, J. High Energy Phys. 10 (2016) 147, arXiv:1607.07655.
[40] J. Heeck, S. Patra, Minimal left-right symmetric dark matter, Phys. Rev. Lett. 115 (12) (2015) 121804, arXiv:1507.01584.

[41] C. Garcia-Cely, J. Heeck, Phenomenology of left-right symmetric dark matter, arXiv:1512.03332, J. Cosmol. Astropart. Phys. 1603 (2016) 021.
[42] S. Patra, S. Rao, Singlet fermion dark matter within left-right model, Phys. Lett. B 759 (2016) 454–458, arXiv:1512.04053.
[43] S. Patra, Dark matter, lepton and baryon number, and left-right symmetric theories, Phys. Rev. D 93 (9) (2016) 093001, arXiv:1512.04739.
[44] F.F. Deppisch, C. Hati, S. Patra, P. Pritimita, U. Sarkar, Neutrinoless double beta decay in left-right symmetric models with a universal seesaw mechanism, Phys. Rev. D 97 (3) (2018) 035005, arXiv:1701.02107.
[45] C. Hati, S. Patra, P. Pritimita, U. Sarkar, Neutrino masses and leptogenesis in left–right symmetric models: a review from a model building perspective, Front. Phys. 6 (2018) 19.
[46] P.S. Bhupal Dev, R.N. Mohapatra, W. Rodejohann, X.-J. Xu, Vacuum structure of the left-right symmetric model, J. High Energy Phys. 02 (2019) 154, arXiv:1811.06869.
[47] G. Chauhan, Vacuum stability and symmetry breaking in left-right symmetric model, J. High Energy Phys. 12 (2019) 137, arXiv:1907.07153.
[48] V. Tello, M. Nemevsek, F. Nesti, G. Senjanovic, F. Vissani, Left-right symmetry: from LHC to neutrinoless double beta decay, Phys. Rev. Lett. 106 (2011) 151801, arXiv:1011.3522.
[49] J. Barry, W. Rodejohann, Lepton number and flavour violation in TeV-scale left-right symmetric theories with large left-right mixing, J. High Energy Phys. 09 (2013) 153, arXiv:1303.6324.
[50] P.S. Bhupal Dev, S. Goswami, M. Mitra, W. Rodejohann, Constraining neutrino mass from neutrinoless double beta decay, Phys. Rev. D 88 (2013) 091301, arXiv:1305.0056.
[51] M. Nemevsek, F. Nesti, G. Senjanovic, Y. Zhang, First limits on left-right symmetry scale from LHC data, Phys. Rev. D 83 (2011) 115014, arXiv:1103.1627.
[52] P.S. Bhupal Dev, C.-H. Lee, R.N. Mohapatra, Leptogenesis constraints on the mass of right-handed gauge bosons, Phys. Rev. D 90 (9) (2014) 095012, arXiv:1408.2820.
[53] S.P. Das, F.F. Deppisch, O. Kittel, J.W.F. Valle, Heavy neutrinos and lepton flavour violation in left-right symmetric models at the LHC, Phys. Rev. D 86 (2012) 055006, arXiv:1206.0256.
[54] S. Bertolini, A. Maiezza, F. Nesti, Present and future K and B meson mixing constraints on TeV scale left-right symmetry, Phys. Rev. D 89 (9) (2014) 095028, arXiv:1403.7112.
[55] M. Dhuria, C. Hati, R. Rangarajan, U. Sarkar, Falsifying leptogenesis for a TeV scale $W_R^{\pm}$ at the LHC, Phys. Rev. D 92 (3) (2015) 031701, arXiv:1503.07198.
[56] D. Borah, S. Patra, P. Pritimita, Sub-dominant type-II seesaw as an origin of non-zero θ_{13} in SO(10) model with TeV scale Z' gauge boson, Nucl. Phys. B 881 (2014) 444–466, arXiv:1312.5885.
[57] J. Chakrabortty, H.Z. Devi, S. Goswami, S. Patra, Neutrinoless double-β decay in TeV scale Left-Right symmetric models, J. High Energy Phys. 08 (2012) 008, arXiv:1204.2527.
[58] F.F. Deppisch, L. Graf, S. Kulkarni, S. Patra, W. Rodejohann, N. Sahu, U. Sarkar, Reconciling the 2 TeV excesses at the LHC in a linear seesaw left-right model, Phys. Rev. D 93 (1) (2016) 013011, arXiv:1508.05940.
[59] C. Majumdar, S. Patra, S. Senapati, U.A. Yajnik, $0\nu\beta\beta$ in left-right theories with Higgs doublets and gauge coupling unification, Nucl. Phys. B 951 (2020) 114875, arXiv:1809.10577.
[60] G. Bambhaniya, P.S.B. Dev, S. Goswami, M. Mitra, The scalar triplet contribution to lepton flavour violation and neutrinoless double beta decay in left-right symmetric model, J. High Energy Phys. 04 (2016) 046, arXiv:1512.00440.
[61] P.S. Bhupal Dev, S. Goswami, M. Mitra, TeV scale left-right symmetry and large mixing effects in neutrinoless double beta decay, Phys. Rev. D 91 (11) (2015) 113004, arXiv:1405.1399.
[62] D. Chang, R.N. Mohapatra, M.K. Parida, Decoupling parity and SU(2)-R breaking scales: a new approach to left-right symmetric models, Phys. Rev. Lett. 52 (1984) 1072.
[63] D. Chang, R.N. Mohapatra, M.K. Parida, A new approach to left-right symmetry breaking in unified gauge theories, Phys. Rev. D 30 (1984) 1052.
[64] D. Borah, S. Patra, U. Sarkar, TeV scale left right symmetry with spontaneous D-parity breaking, Phys. Rev. D 83 (2011) 035007, arXiv:1006.2245.
[65] R.L. Awasthi, M.K. Parida, S. Patra, Neutrino masses, dominant neutrinoless double beta decay, and observable lepton flavor violation in left-right models and SO(10) grand unification with low mass W_R, Z_R bosons, J. High Energy Phys. 08 (2013) 122, arXiv:1302.0672.
[66] S. Patra, P. Pritimita, Post-sphaleron baryogenesis and n - $\overline{n}$ oscillation in non-SUSY SO(10) GUT with gauge coupling unification and proton decay, Eur. Phys. J. C 74 (10) (2014) 3078, arXiv:1405.6836.
[67] C. Arbeláez, M. Hirsch, M. Malinský, J.C. Romão, LHC-scale left-right symmetry and unification, Phys. Rev. D 89 (3) (2014) 035002, arXiv:1311.3228.

[68] M.K. Parida, Vanishing corrections on intermediate scale and implications for unification of forces, Phys. Rev. D 57 (1998) 2736–2742, arXiv:hep-ph/9710246.
[69] B.P. Nayak, M.K. Parida, New mechanism for Type-II seesaw dominance in SO(10) with low-mass Z', RH neutrinos, and verifiable LFV, LNV and proton decay, Eur. Phys. J. C 75 (2015) 183, arXiv:1312.3185.
[70] D. Borah, A. Dasgupta, Charged lepton flavour violcxmation and neutrinoless double beta decay in left-right symmetric models with type I+II seesaw, J. High Energy Phys. 07 (2016) 022, arXiv:1606.00378.
[71] D. Borah, A. Dasgupta, Neutrinoless double beta decay in type I+II seesaw models, J. High Energy Phys. 11 (2015) 208, arXiv:1509.01800.
[72] S. Patra, P. Pritimita, 7 keV sterile neutrino Dark Matter in extended seesaw framework, arXiv:1409.3656.
[73] R. Lal Awasthi, M.K. Parida, Inverse seesaw mechanism in nonsupersymmetric SO(10), proton lifetime, nonunitarity effects, and a low-mass Z' boson, Phys. Rev. D 86 (2012) 093004, arXiv:1112.1826.
[74] P.S.B. Dev, R.N. Mohapatra, TeV scale inverse seesaw in SO(10) and leptonic non-unitarity effects, Phys. Rev. D 81 (2010) 013001, arXiv:0910.3924.
[75] P.S. Bhupal Dev, R.N. Mohapatra, Unified explanation of the $eejj$, diboson and dijet resonances at the LHC, Phys. Rev. Lett. 115 (18) (2015) 181803, arXiv:1508.02277.
[76] R.L. Awasthi, M.K. Parida, S. Patra, Neutrinoless double beta decay and pseudo-Dirac neutrino mass predictions through inverse seesaw mechanism, arXiv:1301.4784.
[77] P. Humbert, M. Lindner, S. Patra, J. Smirnov, Lepton number violation within the conformal inverse seesaw, J. High Energy Phys. 09 (2015) 064, arXiv:1505.07453.
[78] W. Grimus, L. Lavoura, The Seesaw mechanism at arbitrary order: disentangling the small scale from the large scale, J. High Energy Phys. 11 (2000) 042, arXiv:hep-ph/0008179.
[79] M. Mitra, G. Senjanovic, F. Vissani, Neutrinoless double beta decay and heavy sterile neutrinos, Nucl. Phys. B 856 (2012) 26–73, arXiv:1108.0004.
[80] M.K. Parida, S. Patra, Left-right models with light neutrino mass prediction and dominant neutrinoless double beta decay rate, Phys. Lett. B 718 (2013) 1407–1412, arXiv:1211.5000.
[81] ATLAS Collaboration, G. Aad, et al., Search for heavy Majorana neutrinos with the ATLAS detector in pp collisions at $\sqrt{s} = 8$ TeV, J. High Energy Phys. 07 (2015) 162, arXiv:1506.06020.
[82] ATLAS Collaboration, M. Aaboud, et al., Search for heavy Majorana or Dirac neutrinos and right-handed W gauge bosons in final states with two charged leptons and two jets at $\sqrt{s} = 13$ TeV with the ATLAS detector, J. High Energy Phys. 01 (2019) 016, arXiv:1809.11105.
[83] ATLAS Collaboration, M. Aaboud, et al., Search for a right-handed gauge boson decaying into a high-momentum heavy neutrino and a charged lepton in pp collisions with the ATLAS detector at $\sqrt{s} = 13$ TeV, Phys. Lett. B 798 (2019) 134942, arXiv:1904.12679.
[84] CMS Collaboration, A.M. Sirunyan, et al., Search for a heavy right-handed W boson and a heavy neutrino in events with two same-flavor leptons and two jets at $\sqrt{s} = 13$ TeV, J. High Energy Phys. 05 (05) (2018) 148, arXiv:1803.11116.
[85] R.N. Mohapatra, New contributions to neutrinoless double beta decay in supersymmetric theories, Phys. Rev. D 34 (1986) 3457–3461, 778 (1986).
[86] K.S. Babu, R.N. Mohapatra, New vector-scalar contributions to neutrinoless double beta decay and constraints on R-parity violation, Phys. Rev. Lett. 75 (1995) 2276–2279, arXiv:hep-ph/9506354, 813 (1995).
[87] M. Hirsch, H.V. Klapdor-Kleingrothaus, S.G. Kovalenko, New supersymmetric contributions to neutrinoless double beta decay, Phys. Lett. B 352 (1995) 1–7, arXiv:hep-ph/9502315.
[88] M. Hirsch, H.V. Klapdor-Kleingrothaus, S.G. Kovalenko, Supersymmetry and neutrinoless double beta decay, Phys. Rev. D 53 (1996) 1329–1348, arXiv:hep-ph/9502385, 787 (1995).
[89] F.F. Deppisch, M. Hirsch, H. Pas, Neutrinoless double beta decay and physics beyond the standard model, J. Phys. G 39 (2012) 124007, arXiv:1208.0727.
[90] H. Pas, M. Hirsch, H.V. Klapdor-Kleingrothaus, S.G. Kovalenko, A superformula for neutrinoless double beta decay. 2. The short range part, Phys. Lett. B 498 (2001) 35–39, arXiv:hep-ph/0008182.
[91] F. Deppisch, H. Pas, Pinning down the mechanism of neutrinoless double beta decay with measurements in different nuclei, Phys. Rev. Lett. 98 (2007) 232501, arXiv:hep-ph/0612165.
[92] H. Päs, W. Rodejohann, Neutrinoless double beta decay, New J. Phys. 17 (11) (2015) 115010, arXiv:1507.00170.
[93] V. Cirigliano, W. Dekens, J. de Vries, M.L. Graesser, E. Mereghetti, A neutrinoless double beta decay master formula from effective field theory, J. High Energy Phys. 12 (2018) 097, arXiv:1806.02780.
[94] V. Cirigliano, W. Dekens, J. de Vries, M.L. Graesser, E. Mereghetti, Neutrinoless double beta decay in chiral effective field theory: lepton number violation at dimension seven, J. High Energy Phys. 12 (2017) 082, arXiv:1708.09390.

[95] G. Pantis, F. Simkovic, J.D. Vergados, A. Faessler, Neutrinoless double beta decay within QRPA with proton - neutron pairing, Phys. Rev. C 53 (1996) 695–707, arXiv:nucl-th/9612036.
[96] M. Doi, T. Kotani, E. Takasugi, Double beta decay and Majorana neutrino, Prog. Theor. Phys. Suppl. 83 (1985) 1.